The calculation of adiabatic-connection curves from full configuration-interaction densities: Two-electron systems

A. M. Teale,[1,a] S. Coriani,[1,2] and T. Helgaker[1]
[1]*Department of Chemistry, Centre for Theoretical and Computational Chemistry, University of Oslo, P.O. Box 1033, Blindern, N-0315 Oslo, Norway*
[2]*Dipartimento di Scienze Chimiche, Università degli Studi di Trieste, Via Licio Giorgieri 1, I-34127 Trieste, Italy*

(Received 25 November 2008; accepted 27 January 2009; published online 13 March 2009)

The Lieb formulation of density-functional theory is briefly reviewed and its straightforward generalization to arbitrary electron-electron interaction strengths discussed, leading to the introduction of density-fixed and potential-fixed adiabatic connections. An iterative scheme for the calculation of the Lieb functionals under the appropriate constraints is outlined following the direct optimization approach of Wu and Yang [J. Chem. Phys. **118**, 2498 (2003)]. First- and second-order optimization schemes for the calculation of accurate adiabatic-connection integrands are investigated and compared; the latter is preferred both in terms of computational efficiency and accuracy. The scheme is applicable to systems of any number of electrons. However, to determine the accuracy that may be achieved, the present work focuses on two-electron systems for which a number of simplifications may be exploited. The procedure is applied to the helium isoelectronic series and the H_2 molecule. The resulting adiabatic-connection curves yield the full configuration-interaction exchange-correlation energies extrapolated to the basis-set limit. The relationship between the Kohn–Sham and natural orbitals as functions of the electron-electron interaction strength is explored in detail for H_2. The accuracy with which the exchange-correlation contributions to the modified local potential can be determined is discussed. The new accurate adiabatic-connection curves are then compared with some recently investigated approximate forms calculated using accurate full configuration-interaction input data. This study demonstrates that the adiabatic-connection integrand may be determined accurately and efficiently, providing important insights into the link between the Kohn–Sham and traditional quantum-chemical treatments of the exchange-correlation problem in electronic-structure theory. © *2009 American Institute of Physics*.
[DOI: 10.1063/1.3082285]

I. INTRODUCTION

In the past two decades, density-functional theory (DFT) has become established as the most widely used method in computational chemistry. The theory has been put on its most rigorous grounds by Lieb[1] using convex functional analysis (see also Ref. 2). In practice, the success of the theory is reliant on the accurate representation of the unknown exchange-correlation energy E_{xc}. Several classes of approximations exist. Ordered in terms of increasing nonlocality these are: the local density approximation (LDA), the generalized gradient approximations (GGAs), meta-GGAs, (hybrid) functionals dependent on occupied orbitals, and finally (hybrid) functionals dependent on all orbitals. The most widely used functionals at present fall into the GGA and occupied-orbital-dependent hybrid-functional categories. The construction of the latter has been motivated by the study of the adiabatic-connection formula for the exchange-correlation energy,[3–7] which arises from consideration of the link between the Kohn–Sham noninteracting and physical interacting systems as a function of the electronic interaction strength.

A number of studies have examined the adiabatic connection using approximate methods,[8–16] and some high-accuracy studies have been carried out for few-electron atomic systems.[17–21] The purpose of the present paper is to describe the implementation of an iterative procedure for the accurate calculation of the adiabatic connection via the optimization of the Lieb convex conjugate functionals under appropriate constraints. The methodology and implementation are generally applicable, although the present study focuses on two-electron systems (both atomic and molecular) to allow the use of highly accurate calculations for the (partially) interacting systems and a detailed assessment of the accuracy achieved.

In Sec. II, we briefly review the Lieb formulation of DFT, introducing the key functionals to be optimized. The generalization of these functionals to arbitrary interaction strength is then examined and the theory of the adiabatic connection is outlined. An alternative adiabatic connection based on a fixed potential rather than a fixed density is also introduced, arising naturally from the Lieb formulation. The relationship of these connections to perturbation theory is also discussed. In Sec. III, an iterative scheme for the calculation of the adiabatic connection in a finite basis set is given as proposed in Ref. 22. In addition, we pay specific attention

[a]Electronic mail: a.m.teale@kjemi.uio.no. FAX: +47 228 55441.

 © 2009 American Institute of Physics

Downloaded 07 Jun 2013 to 193.157.137.211. This article is copyrighted as indicated in the abstract. Reuse of AIP content is subject to the terms at: http://jcp.aip.org/about/rights_and_permissions

to the implementation of a second-order optimization scheme. In Sec. IV, we compare the first- and second-order iterative optimization schemes and examine their convergence with respect to choice of basis set. The application of an extrapolation scheme for estimation of basis-set-limit adiabatic-connection curves is also presented. In Sec. V, the procedure is applied to the helium isoelectronic series and to the H_2 molecule, the relationship between the Kohn–Sham and natural orbitals is explored in some detail, and the variation in the effective potential with interaction strength is examined. The accurate curves obtained are then compared with those from some recently studied[23,24] approximate forms. Finally, some comparisons are drawn between the density-fixed and potential-fixed adiabatic connections. Concluding remarks and directions for future work are discussed in Sec. VI.

II. THEORETICAL BACKGROUND

A. Lieb's convex conjugate density functional

We now briefly review Lieb's convex-conjugate density functional introducing from the outset the coupling-strength parameter λ. Consider an N-electron system described by the Hamiltonian (in atomic units)

$$\hat{H}_\lambda[v] = \hat{T} + \lambda\hat{W} + \sum_i v(\mathbf{r}_i)$$

$$= -\frac{1}{2}\sum_i \nabla_i^2 + \lambda\sum_{i>j}\frac{1}{r_{ij}} + \sum_i v(\mathbf{r}_i), \tag{1}$$

where v is the external potential and where the two-electron interactions depend linearly on λ. For a fully interacting system, $\lambda=1$; for a noninteracting system, $\lambda=0$. We note that parametrizations connecting the interacting and noninteracting systems in a different manner are also possible. However, we only consider here the linear parametrization given in Eq. (1).

The ground-state energy in the external potential v is given by

$$E_\lambda[v] = \inf_{\hat{\gamma}\to N} \mathrm{Tr}\,\hat{H}_\lambda[v]\hat{\gamma}, \tag{2}$$

where the minimization is over all ensemble density matrices $\hat{\gamma}$ containing N electrons. Since $E_\lambda[v]$ is continuous and concave in v, it may be represented by a convex conjugate functional $F_\lambda[\rho]$ of the conjugate variable ρ, the electron density, as first discussed by Lieb.[1] The conjugate functionals $E_\lambda[v]$ and $F_\lambda[\rho]$ are mutual Legendre–Fenchel transforms

$$F_\lambda[\rho] = \sup_{v\in X^*}\left(E_\lambda[v] - \int \rho(\mathbf{r})v(\mathbf{r})\mathrm{d}\mathbf{r}\right), \tag{3}$$

$$E_\lambda[v] = \inf_{\rho\in X}\left(F_\lambda[\rho] + \int \rho(\mathbf{r})v(\mathbf{r})\mathrm{d}\mathbf{r}\right). \tag{4}$$

The domains X and X^* are reflexive Banach spaces such that $\int\rho(\mathbf{r})v(\mathbf{r})\mathrm{d}\mathbf{r}$ is finite for all $\rho\in X$ and $v\in X^*$. As shown by Lieb, the density functional in Eq. (3) may be expressed as a density-matrix constrained-search functional

$$F_\lambda[\rho] = \inf_{\hat{\gamma}\to\rho} \mathrm{Tr}\,\hat{H}_\lambda[0]\hat{\gamma}, \tag{5}$$

where the minimization is now over all density matrices $\hat{\gamma}$ that yield ρ.

The basic relation between the two conjugate functionals of Eqs. (3) and (4) is Fenchel's inequality, which in the case of $E_\lambda[v]$ and $F_\lambda[\rho]$ takes the form

$$E_\lambda[v] \le F_\lambda[\rho] + \int \rho(\mathbf{r})v(\mathbf{r})\mathrm{d}\mathbf{r} \tag{6}$$

and is valid for all pairs of densities $\rho\in X$ and potentials $v\in X^*$. If a given potential v supports an N-electron ground state, this inequality may be sharpened into an equality by minimizing the right-hand side with respect to ρ, which is equivalent to satisfying the stationary condition (for variations that do not change the particle number)

$$\frac{\delta F_\lambda[\rho]}{\delta\rho(\mathbf{r})} = -v(\mathbf{r}). \tag{7}$$

Alternatively, for a given density ρ that is ensemble v-representable, we may instead begin with Fenchel's inequality [Eq. (6)] in the equivalent form

$$F_\lambda[\rho] \ge E_\lambda[v] - \int \rho(\mathbf{r})v(\mathbf{r})\mathrm{d}\mathbf{r} \tag{8}$$

and arrive at an equality by maximizing the right-hand side with respect to v, which (in the absence of degeneracies) is equivalent to satisfying the stationary condition

$$\frac{\delta E_\lambda[v]}{\delta v(\mathbf{r})} = \rho(\mathbf{r}). \tag{9}$$

Since $E_\lambda[v]$ and $F_\lambda[\rho]$ are concave and convex functionals, respectively, they have at most one stationary point, implying that the conditions in Eqs. (7) and (9) uniquely determine the solution if it exists. Note that at a stationary point, the functional derivatives that appear in the left-hand sides of Eqs. (7) and (9) are each other's inverses, relating ground-state potentials and densities. The two stationary conditions are therefore equivalent and are sometimes known as the reciprocal relations.

B. The adiabatic connection

Let us now consider $E_\lambda[v]$ and $F_\lambda[\rho]$ of Eqs. (2) and (5) for a given external potential v and for a given electron density ρ (not necessarily a conjugate pair) and denote the minimizing density matrices at a given interaction strength $0\le\lambda\le1$ by γ_λ^v and γ_λ^ρ, respectively,

$$E_\lambda[v] = \inf_{\hat{\gamma}\to N} \mathrm{Tr}\,\hat{H}_\lambda[v]\hat{\gamma} = \mathrm{Tr}\,\hat{H}_\lambda[v]\hat{\gamma}_\lambda^v, \tag{10}$$

$$F_\lambda[\rho] = \inf_{\hat{\gamma}\to\rho} \mathrm{Tr}\,\hat{H}_\lambda[0]\hat{\gamma} = \mathrm{Tr}\,\hat{H}_\lambda[0]\hat{\gamma}_\lambda^\rho. \tag{11}$$

Whereas the minimizer $\hat{\gamma}_\lambda^\rho$ always exists, for all ρ and all λ, this is not so for $\hat{\gamma}_\lambda^v$, which exists only for those potentials v that can bind N electrons with interaction strength λ. In the following, however, we assume that the minimizer $\hat{\gamma}_\lambda^v$ exists

Downloaded 07 Jun 2013 to 193.157.137.211. This article is copyrighted as indicated in the abstract. Reuse of AIP content is subject to the terms at: http://jcp.aip.org/about/rights_and_permissions

for all λ. Moreover, we assume that $\hat{\gamma}^v_\lambda$ and $\hat{\gamma}^\rho_\lambda$ are both differentiable with respect to λ in the interval $0 \leq \lambda \leq 1$.

In the interacting case $\lambda > 0$, the minimizations of Eqs. (10) and (11) are difficult many-body problems; in contrast, the noninteracting case $\lambda = 0$ can be solved exactly by expressing $\hat{\gamma}^v_0$ and $\hat{\gamma}^\rho_0$ in terms of orbitals. Let us therefore consider the relationships of $E_\lambda[v]$ and $F_\lambda[\rho]$ to their noninteracting limits $E_0[v]$ and $F_0[\rho]$,

$$E_\lambda[v] = E_0[v] + \int_0^\lambda \frac{dE_\lambda[v]}{d\lambda} d\lambda, \tag{12}$$

$$F_\lambda[\rho] = F_0[\rho] + \int_0^\lambda \frac{dF_\lambda[\rho]}{d\lambda} d\lambda. \tag{13}$$

Applying the Hellmann–Feynman theorem to Eqs. (10) and (11),

$$\frac{dE_\lambda[v]}{d\lambda} = \mathrm{Tr}\ \hat{W}\hat{\gamma}^v_\lambda = \mathcal{W}_\lambda[v], \tag{14}$$

$$\frac{dF_\lambda[\rho]}{d\lambda} = \mathrm{Tr}\ \hat{W}\hat{\gamma}^\rho_\lambda = \mathcal{W}_\lambda[\rho], \tag{15}$$

and introducing explicit expressions for $E_0[v]$ and $F_0[\rho]$, we obtain

$$E_\lambda[v] = \mathrm{Tr}\ \hat{H}_0[v]\hat{\gamma}^v_0 + \int_0^\lambda \mathcal{W}_\lambda[v] d\lambda, \tag{16}$$

$$F_\lambda[\rho] = \mathrm{Tr}\ \hat{H}_0[0]\hat{\gamma}^\rho_0 + \int_0^\lambda \mathcal{W}_\lambda[\rho] d\lambda, \tag{17}$$

which may also be expressed in the form

$$E_\lambda[v] = \mathrm{Tr}\ \hat{H}_\lambda[v]\hat{\gamma}^v_0 + \int_0^\lambda \mathcal{W}_{c,\lambda}[v] d\lambda,$$
$$\mathcal{W}_{c,\lambda}[v] = \mathcal{W}_\lambda[v] - \mathcal{W}_0[v], \tag{18}$$

$$F_\lambda[\rho] = \mathrm{Tr}\ \hat{H}_\lambda[0]\hat{\gamma}^\rho_0 + \int_0^\lambda \mathcal{W}_{c,\lambda}[\rho] d\lambda,$$
$$\mathcal{W}_{c,\lambda}[\rho] = \mathcal{W}_\lambda[\rho] - \mathcal{W}_0[\rho]. \tag{19}$$

In these expressions, the first terms are equal to the exact energies of Eqs. (2) and (5) except that we have replaced the interacting density matrices $\hat{\gamma}^\rho_\lambda$ and $\hat{\gamma}^v_\lambda$ by the corresponding noninteracting matrices $\hat{\gamma}^\rho_0$ and $\hat{\gamma}^v_0$, respectively. These terms thus represent uncorrelated approximations to the true energies and may be explicitly computed from orbitals. The second terms in Eqs. (18) and (19) are correlation corrections, requiring a knowledge of $\hat{\gamma}^\rho_\lambda$ and $\hat{\gamma}^v_\lambda$ for $\lambda > 0$ for their evaluation, as discussed below. For simplicity, we use the same notation for the density- and potential-fixed functionals $\mathcal{W}_\lambda[v]$ and $\mathcal{W}_\lambda[\rho]$, respectively, distinguishing these by their arguments v and ρ.

Whereas the energy expression in Eq. (18) is the starting point for a potential-fixed adiabatic connection and for bare-nucleus (BN) perturbation theory[25] with zero-order term $\mathrm{Tr}\ \hat{H}_\lambda[v]\hat{\gamma}^v_0$, the expression in Eq. (19) is the basis for the density-fixed adiabatic connection and for Görling–Levy (GL) perturbation theory[26,27] with zero-order term $\mathrm{Tr}\ \hat{H}_\lambda[0]\hat{\gamma}^\rho_0$. In the potential-fixed adiabatic connection, we determine $\rho_\lambda[v]$ by minimizing the right-hand side of Fenchel's inequality [Eq. (6)] with respect to ρ for a fixed external potential v and for $0 \leq \lambda \leq 1$; conversely, in the density-fixed adiabatic connection, we determine $v_\lambda[\rho]$ by maximizing Fenchel's inequality in the form of Eq. (8) with respect to v, for a fixed physical density ρ, and for $0 \leq \lambda \leq 1$. Although our focus in this paper is on the usual density-fixed adiabatic connection and its relationship to the construction of Kohn–Sham density functionals, the development of the adiabatic connection in terms of Lieb's theory, where $E_\lambda[v]$ and $F_\lambda[\rho]$ appear as conjugate functionals in Eqs. (3) and (4), leads naturally to the consideration of the alternative adiabatic connection based on a fixed potential v. We therefore also give here some attention to this potential-fixed adiabatic connection, comparing it with the density-fixed connection for some selected systems.

1. Decomposition of the universal density functional $F_\lambda[\rho]$

The universal density functional $F_\lambda[\rho]$ is decomposed in the manner

$$F_\lambda[\rho] = T_s[\rho] + \lambda J[\rho] + \lambda E_x[\rho] + E_{c,\lambda}[\rho], \tag{20}$$

where the noninteracting kinetic-energy functional $T_s[\rho]$, the Coulomb functional $J[\rho]$, the exchange functional $E_x[\rho]$, and correlation functional $E_{c,\lambda}[\rho]$ are given by

$$T_s[\rho] = \mathrm{Tr}\ \hat{H}_0[0]\hat{\gamma}^\rho_0 = \mathrm{Tr}\ \hat{T}\hat{\gamma}^\rho_0 = \min_{\hat{\gamma}\to\rho} \mathrm{Tr}\ \hat{T}\hat{\gamma}, \tag{21}$$

$$J[\rho] = \int\int \rho(\mathbf{r}_1)\rho(\mathbf{r}_2) r_{12}^{-1} d\mathbf{r}_1 d\mathbf{r}_2, \tag{22}$$

$$E_x[\rho] = \mathcal{W}_0[\rho] - J[\rho], \tag{23}$$

$$E_{c,\lambda}[\rho] = \int_0^\lambda \mathcal{W}_{c,\lambda}[\rho] d\lambda. \tag{24}$$

Only the Coulomb term $J[\rho]$ depends on the density ρ in an explicit manner; the remaining three terms depend on ρ implicitly through their dependence on $\hat{\gamma}^\rho_\lambda$. Since the noninteracting kinetic-energy functional $T_s[\rho]$ and the exchange functional $E_x[\rho]$ depend explicitly only on the noninteracting density matrix $\hat{\gamma}^\rho_0$, they are calculated exactly in terms of orbitals in Kohn–Sham theory. The only term that depends explicitly on $\hat{\gamma}^\rho_\lambda$ for $\lambda > 0$ is the correlation functional, which is also the only term that depends in a nontrivial manner on λ, noting that the Coulomb and exchange contributions to $F_\lambda[\rho]$ depend linearly on λ. Indeed, it is the dependence of $E_{c,\lambda}[\rho]$ on λ that constitutes the main interest of this paper.

At this point it is interesting to compare and contrast the Hartree–Fock and Kohn–Sham theories in the present context. Both theories employ a single determinant and because of this their kinetic and exchange energy functionals take the

Downloaded 07 Jun 2013 to 193.157.137.211. This article is copyrighted as indicated in the abstract. Reuse of AIP content is subject to the terms at: http://jcp.aip.org/about/rights_and_permissions

same form. In Hartree–Fock theory the single determinant is used to approximate the physical wave function Ψ_1, and the correlation contribution of Eq. (24) is neglected. The orbitals used in the calculation of the exchange and kinetic energies are then those which arise from the variational optimization of $\mathrm{Tr}\,\hat{H}_1[v]\hat{\gamma}_0^v$. In contrast, Kohn–Sham theory uses the single determinant to construct the physical density ρ and includes the correlation contribution of Eq. (24). The orbitals used to construct the Kohn–Sham noninteracting wave function Ψ_0 arise from the minimization of $E^{\mathrm{KS}}[\rho] = \int \rho(\mathbf{r}) v_s(\mathbf{r}) d\mathbf{r} + F_1[\rho]$, where $F_1[\rho]$ is defined as in Eq. (20) and v_s is the external potential entering the $\lambda=0$ Hamiltonian.

From Eq. (19), we see that $\mathcal{W}_{c,\lambda}[\rho]$ provides the correlation contribution to the two-electron interaction of the electronic system at interaction strength λ and therefore vanishes for the noninteracting system $\mathcal{W}_{c,0}[\rho]=0$. The corresponding representation of the exchange-correlation energy $E_{\mathrm{xc},\lambda}[\rho]$ involves

$$\mathcal{W}_{\mathrm{xc},\lambda}[\rho] = E_x[\rho] + \mathcal{W}_{c,\lambda}[\rho] = \mathcal{W}_\lambda[\rho] - J[\rho], \tag{25}$$

which reduces to the exchange energy in the noninteracting limit. The correlation correction to the kinetic energy is obtained by subtracting the correlation contribution to the two-electron energy from the total correlation energy

$$T_{c,\lambda}[\rho] = E_{c,\lambda}[\rho] - \mathcal{W}_{c,\lambda}[\rho] = \int_0^\lambda (\mathcal{W}_{c,\mu}[\rho] - \mathcal{W}_{c,\lambda}[\rho]) d\mu \tag{26}$$

and is thus also easily extracted from $\mathcal{W}_\lambda[\rho]$.

In the case of degeneracy, the noninteracting density matrix $\hat{\gamma}_0^v$ obtained as the minimizer of $\mathrm{Tr}\,\hat{H}_0[0]\hat{\gamma}_0^\rho$ (the noninteracting kinetic energy) is not uniquely defined—that is, there may exist several minimizing noninteracting density matrices, all giving the same density and noninteracting kinetic energy [Eq. (21)]. In such cases, the exchange and correlation functionals of Eqs. (23) and (24) are separately not uniquely defined, although the combined exchange-correlation energy is in all cases well defined (since the kinetic and Coulomb energies are well defined). Of course, the separation between the exchange and correlation energies may be made unique by minimizing, for example, the exchange energy of Eq. (23) with respect to all density matrices that minimize the noninteracting kinetic energy in Eq. (21).

2. Görling–Levy perturbation theory

We are here interested in the dependence of $E_{c,\lambda}[\rho]$ on λ, which may be expressed in a power series about $\lambda=0$ as

$$E_{c,\lambda}[\rho] = \sum_{n=2}^{\infty} \lambda^n E_{\mathrm{GL}}^{(n)}[\rho], \tag{27}$$

which may or may not converge. The zero-order term vanishes by the definition of Eq. (24) and the first-order term by the Hellmann–Feynman theorem applied to Eq. (19). The nonvanishing second- and higher-order terms are evaluated from GL perturbation theory.[26,27] From the expansion of $E_{c,\lambda}[\rho]$ in Eq. (27), we immediately obtain an expansion of $\mathcal{W}_{c,\lambda}[\rho]$ by differentiation with respect to λ,

$$\mathcal{W}_{c,\lambda}[\rho] = \sum_{n=1}^{\infty} \lambda^n \mathcal{W}_{\mathrm{GL}}^{(n)}[\rho] = \sum_{n=1}^{\infty} \lambda^n (n+1) E_{\mathrm{GL}}^{(n+1)}[\rho]. \tag{28}$$

In particular, the slope of $\mathcal{W}_{c,\lambda}[\rho]$ at $\lambda=0$ (which will be of interest later) is given by $\mathcal{W}_{\mathrm{GL}}^{(1)}[\rho] = 2E_{\mathrm{GL}}^{(2)}[\rho]$, whose computation is discussed below.

In GL theory, we set up a Hamiltonian whose external potential v_λ depends on λ in such a way that the density remains fixed,

$$\hat{H}_\lambda[v_\lambda] = \sum_{n=0}^{\infty} \lambda^n \hat{H}_{\mathrm{GL}}^{(n)}. \tag{29}$$

Let $v_1 = v_{\mathrm{ext}}$ be the external potential due to the nuclei. To determine v_λ at $\lambda \neq 1$, we differentiate Eq. (20) with respect to the density and obtain

$$\frac{\delta F_\lambda[\rho]}{\delta\rho(\mathbf{r})} = \frac{\delta T_s[\rho]}{\delta\rho(\mathbf{r})} + \lambda v_J(\mathbf{r}) + \lambda v_x(\mathbf{r}) + v_{c,\lambda}(\mathbf{r}), \tag{30}$$

where we have introduced the potentials

$$v_J(\mathbf{r}) = \frac{\delta J[\rho]}{\delta\rho(\mathbf{r})}, \quad v_x(\mathbf{r}) = \frac{\delta E_x[\rho]}{\delta\rho(\mathbf{r})}, \quad v_{c,\lambda}(\mathbf{r}) = \frac{\delta E_{c,\lambda}[\rho]}{\delta\rho(\mathbf{r})}. \tag{31}$$

The stationary conditions

$$\frac{\delta F_\lambda[\rho]}{\delta\rho(\mathbf{r})} = -v_\lambda(\mathbf{r}) \quad (\lambda > 0), \tag{32}$$

$$\frac{\delta T_s[\rho]}{\delta\rho(\mathbf{r})} = -v_s(\mathbf{r}) \quad (\lambda = 0) \tag{33}$$

now yield the following relation between the effective potentials of the interacting and noninteracting systems

$$v_\lambda(\mathbf{r}) = v_s(\mathbf{r}) - \lambda v_J(\mathbf{r}) - \lambda v_x(\mathbf{r}) - v_{c,\lambda}(\mathbf{r}), \tag{34}$$

where we note that $v_s(\mathbf{r}) = v_{\mathrm{ext}}(\mathbf{r}) + v_J(\mathbf{r}) + v_x(\mathbf{r}) + v_c(\mathbf{r})$ by setting $\lambda=1$. The asymptotic behavior of v_λ is dominated by the Coulomb and exchange contributions so that

$$v_\lambda(\infty) = -Z/r - (1-\lambda)(N-1)/r \tag{35}$$

for an atom of nuclear charge Z and N electrons.

Having determined v_λ, we may now set up the Hamiltonian operators to order n in GL theory

$$\hat{H}_{\mathrm{GL}}^{(0)} = \hat{T} + \textstyle\sum_i v_s(\mathbf{r}_i), \tag{36}$$

$$\hat{H}_{\mathrm{GL}}^{(1)} = \hat{W} - \textstyle\sum_i v_J(\mathbf{r}_i) - \sum_i v_x(\mathbf{r}_i), \tag{37}$$

$$\hat{H}_{\mathrm{GL}}^{(n)} = -\textstyle\sum_i v_c^{(n)}(\mathbf{r}_i), \quad n \geq 2. \tag{38}$$

The solution of the zero-order system yields the Kohn–Sham eigenvalue problem

Downloaded 07 Jun 2013 to 193.157.137.211. This article is copyrighted as indicated in the abstract. Reuse of AIP content is subject to the terms at: http://jcp.aip.org/about/rights_and_permissions

$$[\hat{T} + v_s(\mathbf{r})]\varphi_p(\mathbf{r}) = \varepsilon_p \varphi_p(\mathbf{r}) \tag{39}$$

and is equivalent to the solution of Eq. (33). The lowest-order term in the GL expansion of the correlation energy is given by

$$E_{\mathrm{GL}}^{(2)}[\rho] = -\sum_{ai} \frac{|\langle a|v_x|i\rangle - \Sigma_j \langle aj|ji\rangle|^2}{\varepsilon_a - \varepsilon_i} - \frac{1}{4}\sum_{abij} \frac{|\langle ij||ab\rangle|^2}{\varepsilon_a + \varepsilon_b - \varepsilon_i - \varepsilon_j}, \tag{40}$$

where $\langle pq|rs\rangle = \int\int \varphi_p^*(\mathbf{r}_1)\varphi_q^*(\mathbf{r}_2) r_{12}^{-1} \varphi_r(\mathbf{r}_1)\varphi_s(\mathbf{r}_2) d\mathbf{r}_1 d\mathbf{r}_2$, $\langle pq||rs\rangle = \langle pq|rs\rangle - \langle pq|sr\rangle$, and where the first term contains the difference between the local and exact exchange expressions.

3. Bare-nucleus perturbation theory

In the case of the potential-fixed adiabatic connection, we likewise expand the energy in orders of λ,

$$E_\lambda[v] = \sum_{n=0}^{\infty} \lambda^n E_{\mathrm{BN}}^{(n)}[v], \tag{41}$$

which by differentiation with respect to λ simultaneously gives an expansion of the adiabatic-connection integrand and therefore

$$\mathcal{W}_\lambda[v] = \sum_{n=2}^{\infty} \lambda^n \mathcal{W}_{\mathrm{BN}}^{(n)}[v] = \sum_{n=2}^{\infty} \lambda^n (n+1) E_{\mathrm{BN}}^{(n+1)}[v]. \tag{42}$$

The Hamiltonian is separated into a zero-order BN contribution and a first-order electron-repulsion contribution[25]

$$\hat{H}_\lambda[v] = \hat{H}_{\mathrm{BN}}^{(0)} + \lambda \hat{H}_{\mathrm{BN}}^{(1)}, \tag{43}$$

$$\hat{H}_{\mathrm{BN}}^{(0)} = \hat{T} + \sum_i v_{\mathrm{ext}}(\mathbf{r}_i), \tag{44}$$

$$\hat{H}_{\mathrm{BN}}^{(1)} = \sum_{i>j} r_{ij}^{-1}. \tag{45}$$

The solution of the zero-order system is given by solving a set of one-electron equations

$$[\hat{T} + v_{\mathrm{ext}}(\mathbf{r})]\varphi_p(\mathbf{r}) = \varepsilon_p \varphi_p(\mathbf{r}), \tag{46}$$

which unlike those in Eq. (39) are noniterative since v_{ext} does not depend on the solution. The zeroth order problems in the GL and BN perturbation theories thus differ only in their choice of local potential. The first- and second-order energies are then given by

$$E_{\mathrm{BN}}^{(1)}[v] = \frac{1}{2}\sum_{ij} \langle ij||ij\rangle, \tag{47}$$

$$E_{\mathrm{BN}}^{(2)}[v] = -\sum_{ai} \frac{|\Sigma_j \langle aj||ij\rangle|^2}{\varepsilon_a - \varepsilon_i} - \frac{1}{4}\sum_{abij} \frac{|\langle ij||ab\rangle|^2}{\varepsilon_a + \varepsilon_b - \varepsilon_i - \varepsilon_j}, \tag{48}$$

where the second-order term differs from the corresponding GL term in that the single-excitation contribution only involves exact exchange and the summations are over BN rather than Kohn–Sham orbitals. The BN perturbation theory then plays the same role for the potential-fixed adiabatic connection as GL theory plays for the density-fixed adiabatic connection.

III. CALCULATION OF THE DENSITY-FIXED ADIABATIC-CONNECTION INTEGRAND

We now turn our attention to the question of how to compute $\mathcal{W}_{c,\lambda}[\rho]$ of Eq. (19) for arbitrary λ values. One approach is to determine the minimizing density matrix $\hat{\gamma}_\lambda^\rho$ of the constrained-search functional in Eq. (5). Alternatively, as pointed out by Wu and Yang,[22] we may determine $\hat{\gamma}_\lambda^\rho$ by determining the maximizing potential v_λ in the Legendre–Fenchel transform in Eq. (3) and then extract the density matrix from $E_\lambda[v_\lambda]$. To see the equivalence of the two schemes, assume that ρ is ensemble v-representable and that the search is over ground-state potentials. We may then write the Lieb functional in the form

$$F_\lambda[\rho] = \max_v \min_\gamma \left(\mathrm{Tr}\, \hat{H}_\lambda[v]\hat{\gamma} - \int \rho(\mathbf{r}) v(\mathbf{r}) d\mathbf{r} \right) = \min_\gamma \left(\mathrm{Tr}\, \hat{H}_\lambda[0]\hat{\gamma} - \int [\rho(\mathbf{r}) - \rho_\gamma(\mathbf{r})] v_\lambda(\mathbf{r}) d\mathbf{r} \right), \tag{49}$$

where v_λ is the maximizing potential and where ρ_γ is the density associated with $\hat{\gamma}$. For this expression to be stationary with respect to variations in v around v_λ, we must have $\rho_\gamma = \rho$. Clearly, therefore, v plays the role of the Lagrange multipliers in a constrained minimization over $\hat{\gamma}$, yielding the constrained-search formula in Eq. (5).

To utilize the Legendre–Fenchel transform of Eq. (3) in practical calculations, we require a method to determine accurately the ground-state energy $E_\lambda[v_\lambda]$ for a given λ and for a given modified external potential v_λ. Also required are the physical density to be used as input and the density for a specific value of λ in some modified external potential. For this purpose, we use the coupled-cluster singles-and-doubles (CCSD) method, which for the two-electron systems discussed in the present paper is equivalent to the full configuration-interaction (FCI) model. We begin by introducing the following expansion for the unknown effective potential

$$v_{\lambda,\mathbf{b}}(\mathbf{r}) = v_{\mathrm{ext}}(\mathbf{r}) + (1-\lambda) v_{\mathrm{ref}}(\mathbf{r}) + \sum_t b_t g_t(\mathbf{r}), \tag{50}$$

where v_{ext} is the usual external potential due to the nuclei, v_{ref} is a fixed reference potential, and the final term is a linear combination of Gaussian functions whose coefficients b_t are to be determined. The role of the reference potential is primarily to provide the correct asymptotic behavior of the modifying potential, as shown in Eq. (35), which would otherwise be determined by the most diffuse function in the set $g_t(\mathbf{r})$. The universal Lieb functional may then be written as

$$F_\lambda[\rho] = \max_{\mathbf{b}} \mathcal{F}_{\lambda,\mathbf{b}}[\rho], \tag{51}$$

Downloaded 07 Jun 2013 to 193.157.137.211. This article is copyrighted as indicated in the abstract. Reuse of AIP content is subject to the terms at: http://jcp.aip.org/about/rights_and_permissions

$$\mathcal{F}_{\lambda,\mathbf{b}}[\rho] = E_\lambda[v_{\lambda,\mathbf{b}}] - \int \rho(\mathbf{r}) v_{\lambda,\mathbf{b}}(\mathbf{r}) d\mathbf{r}. \tag{52}$$

The elements of the gradient $\mathbf{G}$ of $\mathcal{F}_{\lambda,\mathbf{b}}[\rho]$ with respect to variations in the coefficients are then given by

$$G_t = \frac{\partial \mathcal{F}_{\lambda,\mathbf{b}}[\rho]}{\partial b_t} = \int [\rho_{\lambda,\mathbf{b}}(\mathbf{r}) - \rho(\mathbf{r})] g_t(\mathbf{r}) d\mathbf{r}, \tag{53}$$

where $\rho_{\lambda,\mathbf{b}}$ is the density corresponding to the energy $E_\lambda[v_{\lambda,\mathbf{b}}]$.

It is possible to set up an iterative procedure based on the quasi-Newton maximization of $\mathcal{F}_{\lambda,\mathbf{b}}[\rho]$. The calculations use a modified version of the DALTON quantum chemistry program[28] and proceed as follows. First, we run a coupled-cluster calculation for a relaxed (Lagrangian) density matrix with the usual $\lambda=1$ electronic Hamiltonian. This provides a well-defined approximation to the physical interacting density ρ of Eq. (52) to be used in the evaluation of the first derivative in Eq. (53). Second, the coupled-cluster code has been modified so that the two-electron integrals may be scaled by λ and the modifying potential contribution $(1-\lambda)v_{\mathrm{ref}}(\mathbf{r})+\Sigma_t b_t g_t(\mathbf{r})$ is added to the one-electron integrals, allowing us to perform coupled-cluster calculations with general Hamiltonians of the type $\hat{H}_\lambda[v_{\lambda,\mathbf{b}}]$ to generate $E_\lambda[v_{\lambda,\mathbf{b}}]$ in Eq. (52). Initially, the coefficients b_t are chosen to be zero and the relaxed density matrix is calculated; from this and the input density matrix, the derivative of Eq. (53) is calculated. A Broyden–Fletcher–Goldfarb–Shanno (BFGS) update of the Hessian $\mathbf{H}$ (taken initially as the identity matrix) is then performed. At each iteration (n), a new set of coefficients for the next iteration $(n+1)$ is determined from

$$\mathbf{b}^{n+1} = \mathbf{b}^n - \mathbf{H}^{-1}\mathbf{G}. \tag{54}$$

The resulting modifying potential is then added to the one-electron integrals and the procedure is iterated until convergence. This approach assumes a quadratic model for the maximization procedure, thus while $-\mathbf{H}^{-1}\mathbf{G}$ is guaranteed to be an ascent direction (since $\mathbf{H}$ is negative definite), the step length must be adjusted in regions far from the global maximum in order to give an increase in the functional. To accomplish this, an approximate line-search algorithm is used, in which the full Newton step is taken initially and, if the functional $\mathcal{F}_{\lambda,\mathbf{b}}[\rho]$ does not increase, the step is reduced until there is a satisfactory change.

While the BFGS update provides a practical way to perform the optimization procedure, the number of iterations required to achieve reasonable convergence can often be quite large. Since at each iteration we perform at least one coupled-cluster calculation (more if backtracking is required in the line search procedure), it is of paramount importance to attempt to reduce the number of iterations. The most effective way to do this is by providing a more accurate approximation to the Hessian by direct calculation rather than using the iterative BFGS update.

The Hessian, which is the second derivative of $\mathcal{F}_{\lambda,\mathbf{b}}[\rho]$ with respect to the coefficients b_t, can be written as[22]

$$H_{tu} = \int\int g_t(\mathbf{r}') g_u(\mathbf{r}) \frac{\delta\rho(\mathbf{r})}{\delta v(\mathbf{r}')} d\mathbf{r} d\mathbf{r}', \tag{55}$$

where $\delta\rho(\mathbf{r})/\delta v(\mathbf{r}')$ is the time-independent linear response of the many-electron density. This may be written in the spectral representation as[29–31,22]

$$\frac{\delta\rho(\mathbf{r})}{\delta v(\mathbf{r}')} = \sum_m \frac{\langle\Psi_0|\hat{\rho}(\mathbf{r})|\Psi_m\rangle\langle\Psi_m|\hat{\rho}(\mathbf{r}')|\Psi_0\rangle}{E_0 - E_m} + \mathrm{c.c.} \tag{56}$$

We introduce the density operator in second quantization

$$\hat{\rho}(\mathbf{r}) = \sum_{pq} \varphi_p^*(\mathbf{r})\varphi_q(\mathbf{r}) E_{pq} \tag{57}$$

with E_{pq} defined as

$$E_{pq} = a_{p\alpha}^\dagger a_{q\alpha} + a_{p\beta}^\dagger a_{q\beta}, \tag{58}$$

where $a_{p\sigma}^\dagger$ and $a_{q\sigma}$ are the creation and annihilation operators acting on spin orbitals with spatial parts p and q, respectively[32] (a similar definition applies for $\hat{\rho}(\mathbf{r}')$). Then defining the one-electron operators

$$\hat{g}_t(\mathbf{r}) = \sum_{pq} g_{t,pq}(\mathbf{r}) E_{pq} \tag{59}$$

whose matrix elements are

$$g_{t,pq}(\mathbf{r}) = \int \varphi_p^*(\mathbf{r})\varphi_q(\mathbf{r}) g_t(\mathbf{r}) d\mathbf{r}, \tag{60}$$

we obtain each element of the approximate Hessian as a static linear response function with the perturbation operators $\hat{g}_t(\mathbf{r})$ and $\hat{g}_u(\mathbf{r}')$,

$$H_{tu} = \sum_m \frac{\langle\Psi_0|\hat{g}_t(\mathbf{r})|\Psi_m\rangle\langle\Psi_m|\hat{g}_u(\mathbf{r}')|\Psi_0\rangle}{E_0 - E_m} + \mathrm{c.c.} \tag{61}$$

In practice, we have modified the CCSD linear response code in DALTON[28] such that a static linear response function is computed for each given pair $\{t,u\}$ of operators in Eq. (59) to obtain the H_{tu} matrix element. Note that the CCSD linear response function is unrelaxed—that is, orbital relaxation is not taken into account.[33] In this sense, the second derivative above is generally an approximate Hessian, although it is exact in the present two-electron study, where the CCSD approach is equivalent to FCI theory. In the spirit of the optimized-effective-potential (OEP) scheme of Ref. 34, we use this Hessian directly in the quasi-Newton procedure.

At convergence, we calculate the expectation value $\mathcal{W}_\lambda[\rho]=\mathrm{Tr}\,\hat{W}\hat{\gamma}_\lambda^\rho$. Subtraction of the Coulomb energy corresponding to the relaxed density gives $\mathcal{W}_{\mathrm{xc},\lambda}[\rho]$, while further subtraction of $\mathcal{W}_{\mathrm{xc},0}[\rho]$ (i.e., $E_x[\rho]$) gives the correlation contribution $\mathcal{W}_{c,\lambda}[\rho]$. The convergence properties of these procedures are considered in detail in Sec. IV A, where we also consider how the choice of auxiliary basis g_t, reference potential v_{ref}, and regularization procedure in the second-order scheme affect the results.

IV. THE CALCULATION OF ACCURATE ADIABATIC-CONNECTION CURVES

In this section, we present the results for two-electron systems using the scheme outlined in Sec III. By focusing on

Downloaded 07 Jun 2013 to 193.157.137.211. This article is copyrighted as indicated in the abstract. Reuse of AIP content is subject to the terms at: http://jcp.aip.org/about/rights_and_permissions

TABLE I. Comparison of first- and second-order iterative procedures for the calculation of adiabatic-connection curves. Basis set aug-cc-pVXZ. See text for details (atomic units).

Method	λ	X	$\mathcal{F}_{\lambda,\mathbf{b}}[\rho]$	$\mathcal{W}_\lambda[\rho]$	$\Delta J\times 10^5$	$\int \mathcal{W}_{\mathrm{xc},\lambda} d\lambda$	$\|\mathbf{G}\|\times 10^5$	N_{iter}
BFGS	0	2	2.8248	1.0157	5.6	−1.0157	1.58	13
		3	2.8610	1.0230	−2.7	−1.0231	1.58	12
		4	2.8646	1.0239	−0.5	−1.0239	3.55	22
		5	2.8661	1.0243	0.6	−1.0243	1.10	10
		6	2.8666	1.0245	16.6	−1.0244	4.47	4
	1/2	2	3.3238	0.9811	6.0	−1.0503	1.10	12
		3	3.3621	0.9824	−2.7	−1.0636	1.41	12
		4	3.3657	0.9816	−1.1	−1.0662	3.42	22
		5	3.3671	0.9814	−1.5	−1.0673	1.08	9
		6	3.3677	0.9814	10.7	−1.0676	4.83	6
	1	2	3.8065	0.9506	0.0	−1.0808	0.00	1
		3	3.8445	0.9484	0.0	−1.0977	0.00	1
		4	3.8475	0.9467	0.0	−1.1011	0.00	1
		5	3.8488	0.9463	0.0	−1.1024	0.00	1
		6	3.8493	0.9461	0.0	−1.1029	0.00	1
Newton	0	2	2.8248	1.0158	7.0	−1.0157	1.43	4
		3	2.8610	1.0231	3.9	−1.0230	0.17	4
		4	2.8646	1.0239	0.2	−1.0239	0.04	4
		5	2.8661	1.0243	−0.2	−1.0243	0.04	3
		6	2.8666	1.0245	−0.2	−1.0245	0.08	2
	1/2	2	3.3238	0.9811	5.1	−1.0503	0.11	4
		3	3.3621	0.9825	2.9	−1.0636	0.13	4
		4	3.3657	0.9816	0.2	−1.0662	0.03	3
		5	3.3671	0.9814	−0.2	−1.0673	0.03	3
		6	3.3677	0.9813	0.0	−1.0676	0.05	3
	1	2	3.8065	0.9506	0.0	−1.0808	0.00	1
		3	3.8445	0.9484	0.0	−1.0977	0.00	1
		4	3.8475	0.9467	0.0	−1.1011	0.00	1
		5	3.8488	0.9463	0.0	−1.1024	0.00	1
		6	3.8493	0.9461	0.0	−1.1029	0.00	1

two-electron systems, we can accurately assess the quality of the results obtained by comparison with FCI results in the same basis set. We begin by considering calculations for the helium atom in a series of basis sets.

A. Convergence and comparison of the iterative procedures

As outlined in Sec. III, the iterative procedure may be carried out using either a BFGS iterative approach requiring only the evaluation of the derivative in Eq. (53) or by use of an approximate Newton scheme, which in addition requires the more involved calculation of the second derivative in Eq. (55). It is important to establish if the extra effort required in the evaluation of the Hessian is worthwhile in terms of both the time taken to run the calculations and the accuracy with which the maximum of Eq. (51) can be obtained. Furthermore, it is useful to know how sensitive the calculation of the adiabatic-connection integrand is to the choice of basis sets. Since, in the present study, we only consider two-electron systems, we will begin with the previously studied helium atom.[17–19]

Extensive preliminary studies indicated the importance of augmenting the basis set with diffuse functions to obtain accurate FCI results and so Dunning's aug-cc-pV*X*Z family of basis sets[35–37] was chosen. In Table I, we present the results for $2\leq X\leq 6$. The values of the maximized target functional $\mathcal{F}_{\lambda,\mathbf{b}}[\rho]$ are presented and represent our best estimates of the functional $F_\lambda[\rho]$ in Eq. (3) for the ground-state physical density along the adiabatic connection. Also presented are the results for the two-electron energy ($\mathcal{W}_\lambda[\rho]$), the difference between the Coulomb energies of the target FCI density and the optimized density returned from the iterative procedure (ΔJ), the computed value of the adiabatic-connection exchange-correlation integral ($\int \mathcal{W}_{\mathrm{xc},\lambda}[\rho]d\lambda$), the minimum value of the gradient in Eq. (53) obtained ($\|\mathbf{G}\|$), and the number of iterations in which convergence is achieved (N_{iter}). Three values of λ are shown corresponding to the Kohn–Sham system ($\lambda=0$), the partially interacting system in the middle of the connection ($\lambda=1/2$), and the physical system ($\lambda=1$).

Our calculations were considered converged when either the gradient fell below 10^{-6} a.u. or the change in $\mathcal{F}_{\lambda,\mathbf{b}}[\rho]$ between iterations was less than 10^{-8} a.u. In all cases, the primary orbital basis set was also used as the auxiliary expansion set g_t. We have confirmed that changing the auxiliary set g_t to a very large uncontracted set of even-tempered *s*-type functions containing exponents 2^n with $-4\leq n\leq 15$ changes the computed $\mathcal{F}_{\lambda,\mathbf{b}}[\rho]$ values by less than 10^{-4} a.u. for the two largest orbital basis sets employed. The changes for the smaller basis sets are larger at 5×10^{-4} and

Downloaded 07 Jun 2013 to 193.157.137.211. This article is copyrighted as indicated in the abstract. Reuse of AIP content is subject to the terms at: http://jcp.aip.org/about/rights_and_permissions

TABLE II. Components of the FCI and Kohn–Sham energies for the helium atom calculated in the aug-cc-pV*X*Z basis sets with and without extrapolation (atomic units).

	$-E_{\mathrm{HF}}$[a]	$-E_{\mathrm{FCI}}$[b]	T_{FCI}[c]	T_s[d]	T_c[e]	$-E_{ne}$[f]	J[g]	$-E_x$[h]	$-E_{\mathrm{xc}}^{\mathrm{FCI}}$[i]	$-\int \mathcal{W}_{\mathrm{xc},\lambda} d\lambda$
DZ	2.8557	2.8896	2.8559	2.8248	0.0311	6.6961	2.0314	1.0157	1.0497	1.0496
TZ	2.8612	2.9006	2.8961	2.8610	0.0351	6.7451	2.0461	1.0230	1.0625	1.0625
QZ	2.8615	2.9025	2.9008	2.8646	0.0361	6.7500	2.0478	1.0239	1.0650	1.0650
5Z	2.8616	2.9032	2.9025	2.8661	0.0365	6.7520	2.0487	1.0243	1.0660	1.0660
6Z	2.8617	2.9035	2.9032	2.8666	0.0365	6.7527	2.0489	1.0245	1.0663	1.0663
[56][j]	2.8617	2.9038	2.9041	2.8674	0.0367	6.7537	2.0493	1.0246	1.0668	1.0668

[a]Calculated from the Hartree–Fock wave function.
[b]Calculated from the FCI wave function.
[c]Calculated as FCI expectation value of the kinetic-energy operator.
[d]Calculated as $T_w[\rho_{\mathrm{FCI}}]$.
[e]Calculated as $T_{\mathrm{FCI}}-T_s$.
[f]Calculated as $\int \rho_{\mathrm{FCI}}(\mathbf{r})v(\mathbf{r})d\mathbf{r}$.
[g]Calculated as $J[\rho_{\mathrm{FCI}}]$.
[h]Calculated as $-\frac{1}{2}J[\rho_{\mathrm{FCI}}]$.
[i]Calculated as $E_{\mathrm{FCI}}-T_s-J-E_{ne}-E_{nn}$
[j]All energies except E_{HF} have been obtained with a two-point aug-cc-pV[56]Z extrapolation.

2×10^{-4} a.u. for the $X=2$ and $X=3$ basis sets, respectively. In the present work, we have used a Fermi–Amaldi reference potential[38] in the expansion of Eq. (50). However, we have confirmed that the use of a scaled version of this potential, as proposed in Ref. 39, or the potential proposed in Ref. 40, changes the calculated $\mathcal{F}_{\lambda,\mathbf{b}}[\rho]$ values also by less than 10^{-4} a.u. In the second-order optimization scheme we employ a truncated singular-value decomposition (TSVD) to regularize the Hessian of Eq. (55) with a cutoff of 10^{-6} on the singular values. Again lower values change $\mathcal{F}_{\lambda,\mathbf{b}}[\rho]$ by less than the accuracy quoted in Table I.

Comparing the two minimization schemes, it is clear that the BFGS approach did not reach the required gradient tolerance, instead converging on the energy criterion. The number of iterations required to achieve this is variable, but typically between 10 and 20 iterations for the systems here. We have confirmed that for larger systems, this number increases rapidly. Indeed, it is possible to invoke much more stringent convergence criteria on the calculations here—for example, by removing the energy criterion. While this allows one to achieve very low values of the gradient, the number of iterations required becomes excessive, often on the order of 200 even for these simple systems. Given that at each iteration, we must perform a FCI calculation and determine a relaxed density, this can make the first-order scheme impractical.

This behavior led us to consider the implementation of the Hessian discussed in Sec. III. As in the OEP scheme of Ref. 34, the use of a directly computed Hessian significantly reduced the number of iterations, typically by a factor of 3. As was observed for the BFGS case, the gradient criterion was only achieved for aug-cc-pVQZ and larger basis sets. Notably, the values of $\mathcal{F}_{\lambda,\mathbf{b}}[\rho]$, $\mathcal{W}_{\lambda}[\rho]$, and $\int \mathcal{W}_{\mathrm{xc},\lambda}[\rho]\mathrm{d}\lambda$ are relatively insensitive to the choice of minimization scheme. As an alternative check, we present the difference between the Coulomb energies of the FCI density and that returned by the iterative procedure. These values give an indication of the degree of success with which the density is held fixed along the connection. It is noteworthy that the second-order scheme achieved substantially higher accuracy for the larger basis sets since the first-order scheme converged slowly toward the input density with very small changes in $\mathcal{F}_{\lambda,\mathbf{b}}[\rho]$ at each iteration.

B. Accuracy of coupling-strength integration

In Table II, we present the Hartree–Fock and FCI total energies. The components of the FCI energy are presented along with the components of the Kohn–Sham energy calculated from the same density. The exchange-correlation energy is obtained in two ways: first, by subtraction of the other Kohn–Sham energy components from the FCI energy to yield an exact value; second, by integration of the $\mathcal{W}_{\mathrm{xc},\lambda}[\rho]$ curves of Eq. (25) plotted in Fig. 1 as a test of the accuracy of the iterative procedure.

One advantage of studying two-electron systems is that we are able to calculate accurately many Kohn–Sham energy components as simple density functionals directly from the FCI electronic density. Specifically, we take advantage of the following simplifications: the noninteracting kinetic energy $T_s[\rho]$ is for a two-electron system equal to the von Weizsäcker energy $T_w[\rho]=\frac{1}{2}\int|\nabla\rho^{1/2}(\mathbf{r})|^2\mathrm{d}\mathbf{r}$, whereas the exchange energy is related to the Coulomb energy as $E_x[\rho]=-\frac{1}{2}J[\rho]$. These energy components are easily extracted from the FCI calculations at the physical coupling strength. The FCI exchange-correlation energy may then be obtained from the FCI energy directly via

$$E_{\mathrm{xc}}^{\mathrm{FCI}} = E^{\mathrm{FCI}} - T_s[\rho] - J[\rho] - E_{ne}[\rho] - E_{nn}, \tag{62}$$

the latter term being zero for atoms.

If our iterative procedure has been sufficiently accurate in computing the maximum of the functional in Eq. (52), then integration of the curves in Fig. 1 should yield this value. The integration of the curves was carried out using the MATHEMATICA program.[41] A number of interpolation and integration schemes were investigated and the results were found to be insensitive to this choice owing to the rather dense spread of points calculated. Integration of the curves

Downloaded 07 Jun 2013 to 193.157.137.211. This article is copyrighted as indicated in the abstract. Reuse of AIP content is subject to the terms at: http://jcp.aip.org/about/rights_and_permissions

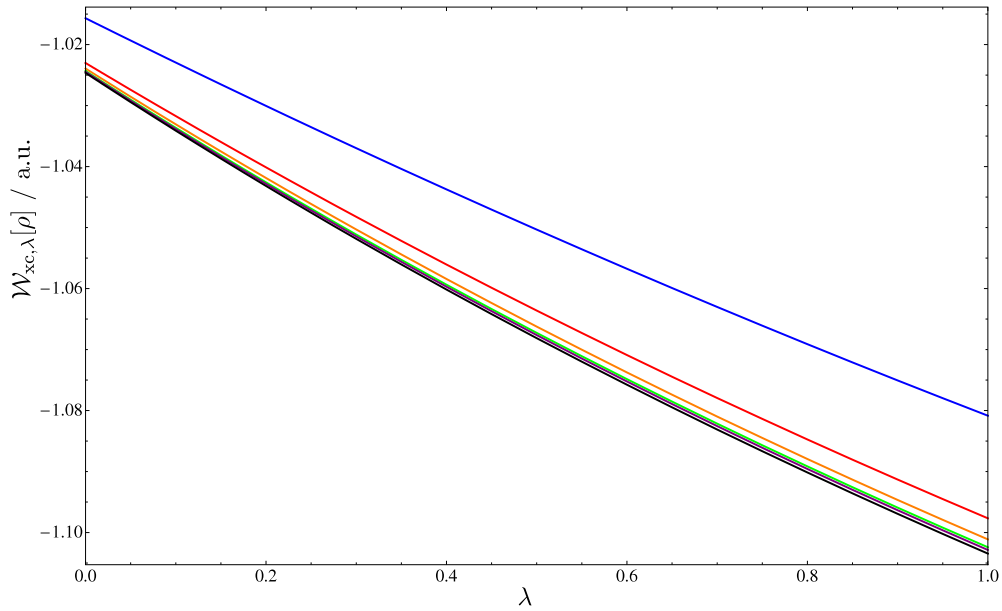

FIG. 1. (Color online) FCI adiabatic-connection curves $\mathcal{W}_{xc,\lambda}[\rho]$ of helium in aug-cc-pVXZ basis sets with $2 \leq X \leq 6$. The curves become more negative as X increases.

for all basis sets shows excellent agreement of better than 10^{-4} a.u. with the accurate E_{xc}^{FCI} values calculated using Eq. (62). The results are presented in Table II.

C. Basis-set convergence of the adiabatic-connection curves

In the FCI calculations, the accuracy obtained depends critically on the quality of the one-electron basis sets in which the wave function is expanded. Moreover, since the basis-set convergence is slow, high accuracy requires the use of large basis sets, combined with extrapolations to the basis-set limit. Here we consider application of the extrapolation scheme presented in Ref. 42 to $\mathcal{W}_{xc,\lambda}[\rho]$ and the energy components presented in Table II. Specifically, we apply the extrapolation

$$E_{XY} = \frac{X^3 E_X - Y^3 E_Y}{X^3 - Y^3}, \tag{63}$$

where X and Y are the cardinal numbers of the two largest basis sets with energies E_X and E_Y, respectively. In Table II, the application of this formula to the FCI expectation values E_{FCI} and T_{FCI} is standard and its efficacy well documented. Its application to $T_s[\rho]$, $E_{ne}[\rho]$, $J[\rho]$, and $E_x[\rho] = -\frac{1}{2}J[\rho]$ is less standard since these terms depend explicitly on the electron density. However, noting that the electron density represents a FCI expectation value of the density operator, it follows that its convergence at each point in space follows the usual X^{-3} expression; it is therefore reasonable to expect that all density functionals should depend in the same manner on the basis set used for the FCI evaluation of the energy. Consequently, we have applied the usual two-point basis-set extrapolation formula in Eq. (63) to these terms. The only term in Table II that does not follow this convergence is the Hartree–Fock energy E_{HF} that converges exponentially; the basis-set limit result of E_{HF} given in the table is based on the assumption of exponential convergence, which incidentally gives here the same result as the (unjustified) application of Eq. (63).

While Tables I and II give an indication of the accuracy achieved numerically, it is interesting to examine visually the behavior of the adiabatic-connection integrand for various values of λ and choices of basis set. Plots of $\mathcal{W}_{xc,\lambda}[\rho]$ along the connection are presented in Fig. 1. The calculations were carried out on a dense grid of points between $\lambda = 0$ and $\lambda = 1$. From Fig. 1, it is clear that the aug-cc-pVDZ basis set is inadequate for the accurate computation of the adiabatic-connection curve. From Eq. (25), we see that $\mathcal{W}_{xc,0}[\rho] = E_x[\rho]$ for the noninteracting system. At all λ values the basis-set convergence is slow. This reflects the slow FCI basis-set convergence of the input physical density matrix. In principle, it would have been possible to use also a different choice of basis set in the calculation of $E_\lambda[v]$ and the calculation of the input physical density ρ of Eq. (52). However, in the present work we choose the same basis set for the input physical density, the potential expansion, and the calculation of $E_\lambda[v]$.

V. APPLICATION TO THE He ISOELECTRONIC SERIES AND TO H_2

In this section, the iterative procedure is applied to the helium isoelectronic series and the H_2 molecule. The relationship between the Kohn–Sham and natural orbitals is explored and the exchange-correlation contributions to the external potential are investigated.

A. The helium isoelectronic series: H^- to Ne^{8+}

The helium isoelectronic series has been extensively studied and poses a significant challenge for approximate exchange-correlation functionals, particularly as Z increases.[17,18,43–47] To be consistent across the series, the uncontracted aug-cc-pCVXZ basis sets[35–37,48] are employed,

Downloaded 07 Jun 2013 to 193.157.137.211. This article is copyrighted as indicated in the abstract. Reuse of AIP content is subject to the terms at: http://jcp.aip.org/about/rights_and_permissions

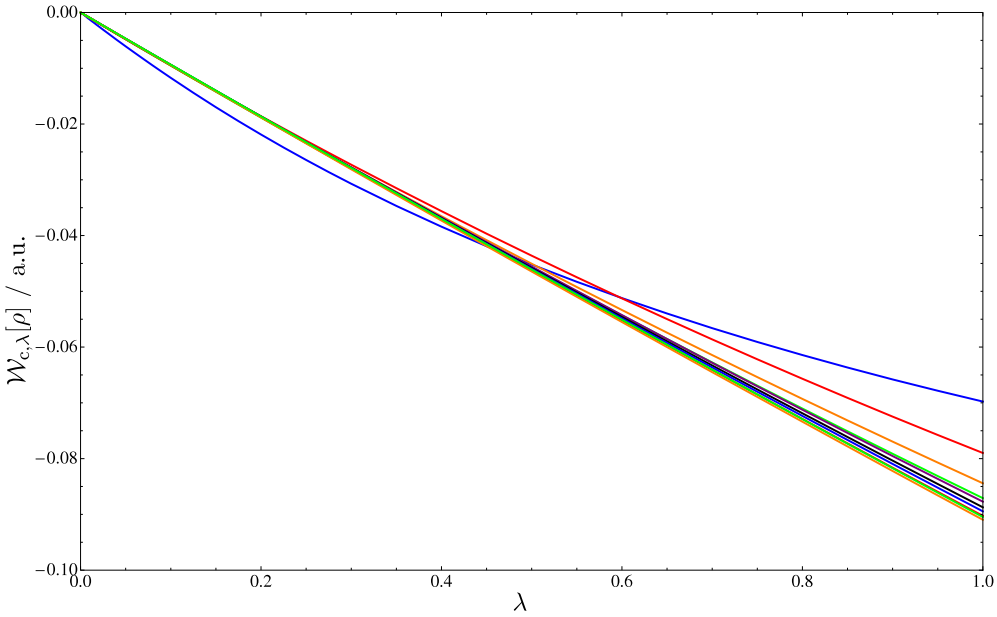

FIG. 2. (Color online) Basis-set limit adiabatic-connection curves of $\mathcal{W}_{c,\lambda}[\rho]$ for the helium isoelectronic series. The curves may be distinguished by noting that $\mathcal{W}_{c,1}[\rho]$ becomes more negative with increasing nuclear charge $1 \leq Z \leq 10$.

noting that uncontraction is essential to describe accurately the compact densities as Z increases. Basis-set extrapolated $\mathcal{W}_{c,\lambda}[\rho]$ curves are presented in Fig. 2 (For easier comparison of curves with different Z, we consider here $\mathcal{W}_{c,\lambda}[\rho]$ which does not contain the exchange contribution present in $\mathcal{W}_{\mathrm{xc},\lambda}[\rho]$ plotted in Fig. 1). The energy components including exchange-correlation energies obtained by integration of the curves are presented in Table III.

The extrapolated curves presented in Fig. 2 are visually indistinguishable from the best approximate curves presented in our recent work on the adiabatic connection.[24] Notably the H^- ion stands out as having far greater curvature than the other members of the series. To understand this behavior, let $\rho(\mathbf{r})$ be the density of H^-. To a reasonably good approximation, the density of the isoelectronic series is then given by $\rho_Z(\mathbf{r}) \approx Z^3\rho(Z\mathbf{r})$, which is equivalent to a scaling of the density of H^-. From the general scaling relationship $E_{c,\lambda}[\rho] = \lambda^2 E_c[\rho_{1/\lambda}]$,[49] it then follows that $E_c[\rho_Z] \approx Z^2 E_{c,1/Z}[\rho]$. For larger and larger Z, therefore, the adiabatic connection effectively explores a smaller and smaller λ interval of some approximately universal adiabatic-connection curve valid for all Z. Consequently, these curves become more linear with increasing charge as the system approaches the high-density limit where the electron-electron interaction is a weak perturbation.[8,15,26,27,47,50–52] The trend toward this linearity and the rate at which it occurs are clear in Fig. 2.

In Table III, we present the numerical values of each component and our extrapolated estimates of the basis-set limit. The first two columns show the Hartree–Fock and FCI energies. The rapid convergence of the former and the slower convergence of the latter are clearly evident. The extrapolated energies all agree to better than 5×10^{-4} a.u. with the accurate values in Ref. 44. The next three columns display the components of the FCI energy $E_{\mathrm{FCI}} = T_{\mathrm{FCI}}[\rho] + \mathcal{W}_1[\rho] + E_{ne}[\rho]$; the slow basis-set convergence is again clear for the kinetic term $T_{\mathrm{FCI}}[\rho]$, the electron-nuclear term E_{ne}, and two-electron term $\mathcal{W}_1[\rho]$. The next three columns give Kohn–Sham energy components: the noninteracting kinetic-energy contribution $T_s[\rho]$, the Coulomb energy $J[\rho]$, and the exchange energy $E_x[\rho]$, all calculated as described in Sec. IV B. Basis-set extrapolation has been applied in the same manner as discussed previously in Table II. The accurate exchange-correlation energies are presented in the penultimate column. The integration of the basis-set extrapolated curves compared with the similarly extrapolated $E_{\mathrm{xc}}^{\mathrm{FCI}}[\rho]$ values leads to errors on the same order as those observed for the total energies. All values agree to better than 5×10^{-4} a.u. except for Li^+ and Be^{2+}. The larger errors for these two species result from the fact that the largest basis sets available were for cardinal numbers 3 and 4, and so only less accurate extrapolations could be performed. We stress, however, that the iterative procedure provides adiabatic-connection curves that reproduce the FCI energy to better than 10^{-4} a.u. in all basis sets. We can now be confident that our calculated curves represent accurate approximations to the true adiabatic-connection curves and that the extrapolated curves are reasonable estimates of the basis-set limit curves (to an error less than 10^{-3} a.u.). Moreover, the curves reproduce the rapid progression toward the linearity expected as we approach the high-density regime.

B. The H_2 molecule

The H_2 molecule is a prototypical system which can be considered as representative for the dissociation of electron-pair bonds in general. However, the accurate calculation of the H_2 dissociation curve is a substantial challenge within DFT. The dilemma for Kohn–Sham calculations is whether or not to employ a spin-restricted formalism. For the true interacting system, the ground-state wave function Ψ_1 is always a singlet.[53] In Kohn–Sham calculations, we may choose whether to enforce spin symmetry by working in a

Downloaded 07 Jun 2013 to 193.157.137.211. This article is copyrighted as indicated in the abstract. Reuse of AIP content is subject to the terms at: http://jcp.aip.org/about/rights_and_permissions

TABLE III. FCI and Kohn–Sham energy components for the helium isoelectronic series in the uncontracted aug-cc-pCV*X*Z basis sets with and without extrapolation (atomic units); for explanations of terms, see Table II.

	Basis	$-E_{\mathrm{HF}}$	$-E_{\mathrm{FCI}}$	$T_{\mathrm{FCI}}[\rho]$	$-E_{ne}[\rho]$	$\mathcal{W}_1[\rho]$	$T_s[\rho]$	$J[\rho]$	$-E_x[\rho]$	$-E_{\mathrm{xc}}^{\mathrm{FCI}}[\rho]$	$-\int \mathcal{W}_{\mathrm{xc},\lambda}[\rho]d\lambda$
H^-	DZ	0.4872	0.5245	0.5300	1.3774	0.3229	0.5020	0.7794	0.3897	0.4285	0.4285
	TZ	0.4877	0.5266	0.5301	1.3751	0.3184	0.5020	0.7740	0.3870	0.4276	0.4276
	QZ	0.4878	0.5271	0.5300	1.3744	0.3173	0.5020	0.7726	0.3863	0.4273	0.4273
	5Z	0.4879	0.5274	0.5293	1.3720	0.3153	0.5013	0.7692	0.3846	0.4260	0.4260
	[Q5]	0.4880	0.5277	0.5286	1.3695	0.3132	0.5007	0.7657	0.3828	0.4246	0.4241
He	DZ	2.8557	2.8910	2.8666	6.7076	0.9499	2.8343	2.0354	1.0177	1.0531	1.0531
	TZ	2.8612	2.9011	2.8967	6.7455	0.9477	2.8611	2.0464	1.0232	1.0632	1.0632
	QZ	2.8615	2.9027	2.9012	6.7505	0.9466	2.8650	2.0482	1.0241	1.0653	1.0653
	5Z	2.8616	2.9032	2.9027	6.7521	0.9462	2.8662	2.0487	1.0244	1.0660	1.0660
	[Q5]	2.8617	2.9038	2.9042	6.7538	0.9459	2.8675	2.0493	1.0246	1.0668	1.0670
Li^+	DZ	7.2361	7.2723	7.2609	16.1121	1.5788	7.2267	3.2986	1.6493	1.6855	1.6855
	TZ	7.2364	7.2774	7.2751	16.1240	1.5715	7.2369	3.3014	1.6507	1.6917	1.6917
	QZ	7.2364	7.2787	7.2775	16.1257	1.5695	7.2384	3.3018	1.6509	1.6932	1.6932
	[TQ]	7.2364	7.2796	7.2793	16.1269	1.5680	7.2395	3.3020	1.6510	1.6943	1.6952
Be^{2+}	DZ	13.6108	13.6474	13.6370	29.4882	2.2038	13.6019	4.5510	2.2755	2.3121	2.3121
	TZ	13.6112	13.6527	13.6506	29.4987	2.1953	13.6111	4.5528	2.2764	2.3180	2.3180
	QZ	13.6113	13.6543	13.6537	29.5009	2.1929	13.6131	4.5530	2.2765	2.3195	2.3195
	[TQ]	13.6113	13.6554	13.6560	29.5025	2.1912	13.6146	4.5532	2.2766	2.3207	2.3217
B^{3+}	DZ	21.9855	22.0222	22.0112	46.8622	2.8287	21.9756	5.8021	2.9010	2.9378	2.9378
	TZ	21.9857	22.0275	22.0239	46.8711	2.8197	21.9838	5.8033	2.9017	2.9435	2.9435
	QZ	21.9862	22.0296	22.0283	46.8748	2.8170	21.9868	5.8036	2.9018	2.9452	2.9452
	5Z	21.9862	22.0303	22.0298	46.8760	2.8158	21.9879	5.8038	2.9019	2.9459	2.9460
	[Q5]	21.9863	22.0311	22.0315	46.8772	2.8146	21.9889	5.8039	2.9020	2.9467	2.9470
C^{4+}	DZ	32.3602	32.3971	32.3854	68.2360	3.4535	32.3495	7.0527	3.5264	3.5633	3.5633
	TZ	32.3604	32.4022	32.3969	68.2436	3.4445	32.3564	7.0536	3.5268	3.5686	3.5687
	QZ	32.3611	32.4047	32.4030	68.2491	3.4414	32.3610	7.0540	3.5270	3.5706	3.5706
	5Z	32.3612	32.4055	32.4048	68.2505	3.4402	32.3623	7.0541	3.5271	3.5714	3.5714
	[Q5]	32.3613	32.4063	32.4068	68.2520	3.4389	32.3636	7.0543	3.5271	3.5722	3.5725
N^{5+}	DZ	44.7348	44.7717	44.7591	93.6092	4.0784	44.7229	8.3031	4.1516	4.1886	4.1886
	TZ	44.7351	44.7765	44.7694	93.6161	4.0702	44.7291	8.3037	4.1519	4.1933	4.1933
	QZ	44.7360	44.7798	44.7776	93.6234	4.0660	44.7353	8.3042	4.1521	4.1959	4.1959
	5Z	44.7361	44.7806	44.7799	93.6252	4.0647	44.7369	8.3044	4.1522	4.1967	4.1967
	[Q5]	44.7362	44.7815	44.7822	93.6270	4.0633	44.7385	8.3046	4.1523	4.1976	4.1979
O^{6+}	DZ	59.1093	59.1463	59.1319	122.9816	4.7034	59.0957	9.5534	4.7767	4.8137	4.8137
	TZ	59.1098	59.1509	59.1432	122.9898	4.6956	59.1030	9.5540	4.7770	4.8181	4.8182
	QZ	59.1110	59.1547	59.1520	122.9976	4.6910	59.1095	9.5544	4.7772	4.8209	4.8209
	5Z	59.1111	59.1557	59.1548	122.9999	4.6894	59.1115	9.5546	4.7773	4.8219	4.8219
	[Q5]	59.1112	59.1568	59.1578	123.0023	4.6877	59.1136	9.5548	4.7774	4.8230	4.8233
F^{7+}	DZ	75.4838	75.5207	75.5046	156.3538	5.3285	75.4683	10.8035	5.4018	5.4387	5.4387
	TZ	75.4844	75.5255	75.5172	156.3634	5.3208	75.4769	10.8042	5.4021	5.4432	5.4432
	QZ	75.4859	75.5296	75.5266	156.3722	5.3160	75.4840	10.8046	5.4023	5.4460	5.4460
	5Z	75.4861	75.5308	75.5297	156.3746	5.3141	75.4862	10.8047	5.4024	5.4471	5.4471
	[Q5]	75.4863	75.5321	75.5330	156.3772	5.3121	75.4884	10.8049	5.4025	5.4483	5.4486
Ne^{8+}	DZ	93.8582	93.8951	93.8769	193.7255	5.9535	93.8405	12.0537	6.0268	6.0638	6.0638
	TZ	93.8590	93.9001	93.8912	193.7370	5.9458	93.8509	12.0543	6.0272	6.0683	6.0683
	QZ	93.8608	93.9046	93.9015	193.7469	5.9408	93.8587	12.0547	6.0274	6.0711	6.0711
	5Z	93.8611	93.9058	93.9046	193.7494	5.9390	93.8609	12.0549	6.0274	6.0722	6.0722
	[Q5]	93.8613	93.9071	93.9079	193.7520	5.9370	93.8633	12.0550	6.0275	6.0733	6.0737

restricted formalism. In the restricted case, we determine a self-consistent solution for which $\rho_\alpha(\mathbf{r})=\rho_\beta(\mathbf{r})=\rho(\mathbf{r})/2$. This is consistent with the physical picture for a singlet wave function. However, the requirement of spin symmetry leads to an unsatisfactory dissociation curve. In Fig. 3, we present the FCI, Hartree–Fock, and Becke–3–Lee–Yang–Parr (B3LYP) potential-energy curves calculated using a restricted formalism. At equilibrium and short internuclear separations R, the B3LYP potential is an improvement over the Hartree–Fock potential and agrees well with the FCI potential. However, as R increases, the accuracy rapidly deteriorates, resulting in a poor molecular dissociation energy. For the restricted Hartree–Fock (RHF) wave function, this may be understood in terms of unphysical ionic contributions ($H^+ \ldots H^-$) that are not present in the Heitler–London wave function.

The alternative is to relax the spin-symmetry constraint in Kohn–Sham calculations by utilizing an unrestricted for-

Downloaded 07 Jun 2013 to 193.157.137.211. This article is copyrighted as indicated in the abstract. Reuse of AIP content is subject to the terms at: http://jcp.aip.org/about/rights_and_permissions

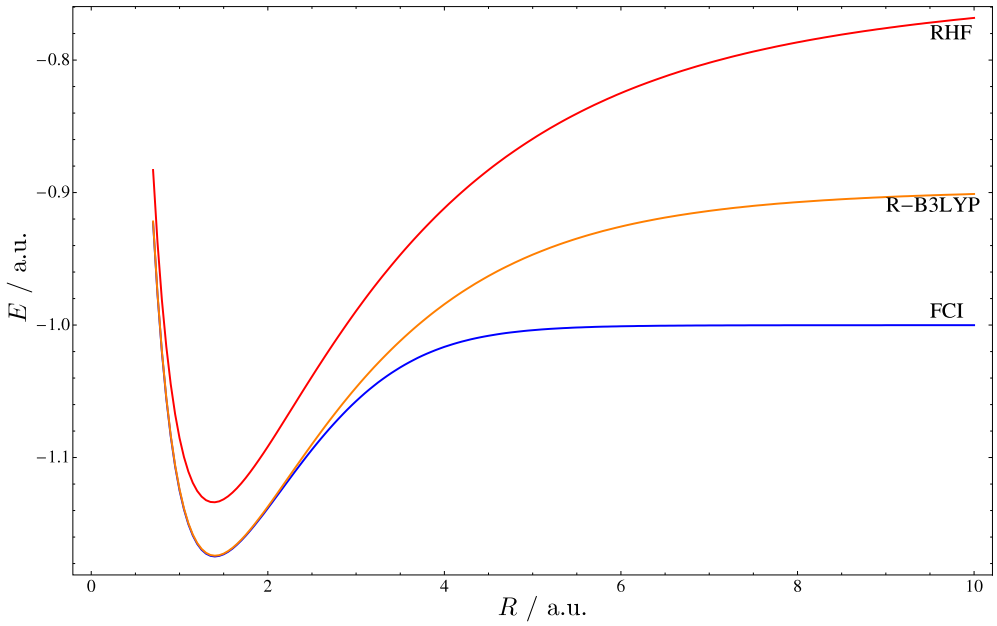

FIG. 3. (Color online) Potential-energy curves for the dissociation of H_2. The curves presented are extrapolated from aug-cc-pVQZ and aug-cc-pV5Z results.

malism (not presented). In this case, as R increases, the potential-energy curves can be in excellent agreement with the FCI results. However, this success comes at a price. In unrestricted Hartree–Fock (UHF) theory, the wave function agrees with the RHF one at short and equilibrium bond lengths; as R increases, they begin to differ and the previously mentioned ionic contributions raise the RHF energy. Meanwhile, the UHF energy begins to become accurate compared with the FCI values. However, the wave function becomes spin contaminated—that is, it is no longer a pure singlet state. In unrestricted Kohn–Sham calculations, the focus is on the density and spin densities. Here the problem manifests itself as a localization of ρ_α on one hydrogen atom and ρ_β on the other (the same is observed for the UHF densities). Whereas the total energy is reasonable, the spin densities are inconsistent with a singlet ground state (although the total density may be remarkably accurate, a fact exploited in Ref. 10).

In fact, as $R \to \infty$, we should obtain two spin-unpolarized hydrogen atoms, the energy of which is degenerate with two infinitely separated spin-polarized hydrogen atoms. While some recent progress has been made in developing exchange-correlation functionals to address this long standing problem,[54–56] significant challenges remain. One route to further understanding the role of DFT exchange and correlation in the H_2 molecule is through investigation of the adiabatic connection, linking the singlet spin-unpolarized exact ground state system to the noninteracting Kohn–Sham single determinant. Following recent work in this direction,[10,23,24] we now apply the iterative procedure of Sec. III to the calculation of accurate adiabatic-connection curves at $R = 0.7, 1.4, 3.0, 5.0, 7.0$ and 10.0 bohr. Again, basis-set extrapolation is applied and the resulting $\mathcal{W}_{c,\lambda}[\rho]$ curves are presented in Fig. 4. The components of the FCI and Kohn–Sham energies are presented in Table IV. For these singlet ground-state H_2 calculations, the standard aug-cc-pVXZ basis sets of Dunning and co-workers[35–37] were employed. A restricted formalism was used throughout. The extrapolated FCI energies in Table IV may be compared with the accurate values in Refs. 57 and 58 and agree to better than 2.5×10^{-4} a.u. (although the values in the present work are consistently lower).

We now make some comments on the shapes of the extrapolated $\mathcal{W}_{c,\lambda}[\rho]$ curves in Fig. 4. Consistent with the helium curves presented in the Sec. IV C, the curvature for the $R=0.7$ bohr plot is subtle. Only a slight increase is observed in moving to the near equilibrium geometry of $R=1.4$ bohr. For the remaining curves as R increases, the curvature increases quite rapidly. In fact, as $R \to \infty$, the curve would become a horizontal line at the exchange energy of an isolated hydrogen atom. The integrals of the curves presented are the Kohn–Sham correlation energies at each geometry. The exchange-correlation energy of the H_2 molecule at dissociation is thus twice the exchange energy of an isolated hydrogen atom and exactly cancels the Coulomb-energy contribution as required. This happens since the H_2 molecule dissociates into one-electron fragments for which there is no correlation energy and the kinetic-correlation energy contribution T_c is zero. In this respect, the H_2 molecule is a special case since for typical molecules the dissociated fragments will contain correlation in either one or both parts, and therefore T_c will not be zero. Qualitatively, the shape of the curves is consistent with those resulting from the most accurate approximate $\mathcal{W}_{\mathrm{xc},\lambda}[\rho]$ forms presented in our previous works.[23,24] Explicit comparisons with these forms are presented in Sec. V E.

In terms of basis-set convergence of the $\mathcal{W}_{\mathrm{xc},\lambda}[\rho]$ curves, the behavior at $R=0.7$ and 1.4 bohr is similar to that observed for helium in Sec. IV C. However, as the bond is stretched, the dynamic correlation becomes negligible and only static correlation remains. Interestingly then, on the scale of Fig. 4, the curves for the three largest basis sets at 3.0, 5.0, 7.0, and 10.0 bohr are essentially indistinguishable

Downloaded 07 Jun 2013 to 193.157.137.211. This article is copyrighted as indicated in the abstract. Reuse of AIP content is subject to the terms at: http://jcp.aip.org/about/rights_and_permissions

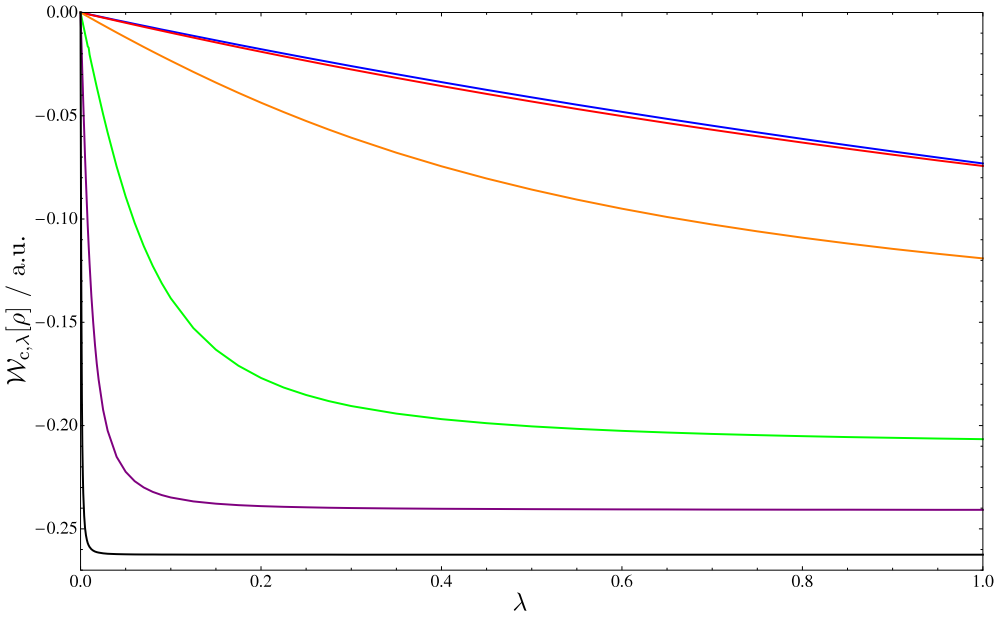

FIG. 4. (Color online) Adiabatic-connection curves for the H_2 molecule at a range of internuclear separations. $R=0.7$, 1.4, 3.0, 5.0, 7.0, and 10.0 bohr from top to bottom.

from the extrapolated curves. This may be expected as the slow basis-set convergence of correlated calculations is associated with the description of the electron-electron cusp.

C. The relationship between Kohn–Sham and natural orbitals

One may be interested in the relationship between the Kohn–Sham orbitals and the natural orbitals of the FCI density for a given coupling strength. Figure 5 presents the natural-orbital occupations for the $1\sigma_g$ and $1\sigma_u$ orbitals along the adiabatic connection for the six geometries of H_2 considered with the largest basis set employed. These natural orbitals are the dominant ones in H_2 and are responsible for the left-right correlation, which is of interest to us here; the higher occupation numbers refine the picture but are of less importance and are therefore omitted. The change in the density matrix along the adiabatic connection reflects the change in the nature of the wave function and the increasing nonlocality of the potential contribution in the Hamiltonian of Eq. (1). The extension of the Hohenberg–Kohn theorem to nonlocal potentials was given by Gilbert[59] and the electronic energy as a functional of the reduced one-electron density matrix was discussed in Ref. 60.

The resemblance of these curves to those of the adiabatic connection is striking. At short and equilibrium geometries, the natural occupation numbers deviate little from the values of two and zero as the coupling strength is increased, indicating the absence of static correlation at these distances. However, as the bond is stretched, the occupation numbers at full coupling strength fall below two and rise above zero considerably; by $R=10.0$ bohr, they are approaching one in each orbital, consistent with the fact that at dissociation we must have two degenerate hydrogen atoms each with a one electron density, the square root of which will be the singly occupied orbital. This behavior is well known. The new information in Fig. 5 is the rate at which the occupation numbers deviate from the Kohn–Sham values toward those of the FCI calculation as the electron-electron interaction is switched on. Not only does the deviation from the Kohn–Sham occupation increase as the bond is stretched and static correlation dominates, so too does the rate at which the final values are approached.

It is instructive to consider the effect of employing a finite basis set. In the iterative procedure of Sec. III, we minimize the norm of the derivative in Eq. (53). In a complete basis set, minimization of this expression would ensure that $\rho_{\lambda,\mathbf{b}}(\mathbf{r})-\rho(\mathbf{r})=0$, where the densities in each case are the diagonal element of the one-electron density matrix from the iterative procedure with a given coupling strength and that at the physical value. In a finite basis set, however, we may rewrite Eq. (53) as

$$G_t = \int (D^{\lambda,\mathbf{b}}_{\alpha\beta} - D_{\alpha\beta})\,\eta_\alpha(\mathbf{r})\,\eta_\beta(\mathbf{r})\,g_t(\mathbf{r})\,d\mathbf{r}, \tag{64}$$

where $D^{\lambda,\mathbf{b}}_{\alpha\beta}$ is the density matrix at some iteration of the procedure, $D_{\alpha\beta}$ is the input physical density matrix, η_α and η_β are the atomic basis functions, and g_t are the auxiliary potential-expansion functions.

Let us now consider the $\lambda=0$ case in a finite basis. When no electron-electron interactions are present, the Hamiltonian in Eq. (1) becomes the Kohn–Sham Hamiltonian. The effective potential is purely local and the density matrix $D^{\lambda,\mathbf{b}}_{\alpha\beta}$ will be that of a Kohn–Sham calculation yielding the physical density. The occupation numbers will be two and zero for occupied and unoccupied orbitals, respectively. The FCI density matrix, on the other hand, has nonintegral occupation numbers as discussed above. As shown by Harriman,[61,62] the density uniquely determines the density matrix provided the

Downloaded 07 Jun 2013 to 193.157.137.211. This article is copyrighted as indicated in the abstract. Reuse of AIP content is subject to the terms at: http://jcp.aip.org/about/rights_and_permissions

TABLE IV. FCI and Kohn–Sham energy components for the H_2 molecule at a range of internuclear separations in the aug-cc-pV*X*Z basis sets. All quantities are in atomic units.

Basis	$-E_{\mathrm{HF}}$	$-E_{\mathrm{FCI}}$	$T[\rho]$	$E_{ne}[\rho]$	$\mathcal{W}_1[\rho]$	$T_s[\rho]$	$J[\rho]$	$-E_x[\rho]$	$-E_{\mathrm{xc}}^{\mathrm{FCI}}[\rho]$	$-\int \mathcal{W}_{\mathrm{xc},\lambda}[\rho]d\lambda$
$R=0.7$										
DZ	0.8514	0.8806	1.5824	4.6415	0.7499	1.5567	1.6099	0.8049	0.8343	0.8342
TZ	0.8793	0.9165	1.7446	4.8456	0.7559	1.7123	1.6508	0.8254	0.8626	0.8626
QZ	0.8821	0.9208	1.7646	4.8690	0.7550	1.7315	1.6535	0.8267	0.8654	0.8654
5Z	0.8825	0.9216	1.7675	4.8725	0.7548	1.7342	1.6544	0.8272	0.8663	0.8663
[Q5]	0.8829	0.9225	1.7705	4.8762	0.7546	1.7370	1.6553	0.8277	0.8673	0.8672
$R=1.4$										
DZ	1.1288	1.1646	1.1338	3.6044	0.5917	1.1032	1.3163	0.6582	0.6941	0.6943
TZ	1.1330	1.1726	1.1707	3.6459	0.5882	1.1380	1.3216	0.6608	0.7006	0.7006
QZ	1.1335	1.1739	1.1738	3.6496	0.5876	1.1408	1.3225	0.6613	0.7019	0.7019
5Z	1.1336	1.1743	1.1747	3.6507	0.5875	1.1416	1.3230	0.6615	0.7024	0.7024
[Q5]	1.1337	1.1747	1.1756	3.6519	0.5874	1.1424	1.3234	0.6617	0.7028	0.7028
$R=3.0$										
DZ	0.9880	1.0533	0.8675	2.6143	0.3601	0.8272	0.9520	0.4760	0.5515	0.5512
TZ	0.9890	1.0563	0.8694	2.6176	0.3585	0.8276	0.9538	0.4769	0.5535	0.5535
QZ	0.9893	1.0570	0.8705	2.6193	0.3585	0.8285	0.9546	0.4773	0.5541	0.5541
5Z	0.9893	1.0572	0.8707	2.6197	0.3585	0.8287	0.9548	0.4774	0.5543	0.5543
[Q5]	0.9893	1.0574	0.8710	2.6202	0.3584	0.8289	0.9550	0.4775	0.5545	0.5545
$R=5.0$										
DZ	0.8580	1.0021	0.9723	2.3777	0.2033	0.9504	0.8182	0.4091	0.5930	0.5918
TZ	0.8591	1.0033	0.9744	2.3810	0.2033	0.9522	0.8193	0.4096	0.5938	0.5936
QZ	0.8593	1.0036	0.9750	2.3819	0.2033	0.9527	0.8195	0.4098	0.5940	0.5940
5Z	0.8594	1.0038	0.9753	2.3823	0.2033	0.9529	0.8196	0.4098	0.5940	0.5940
[Q5]	0.8595	1.0039	0.9755	2.3826	0.2033	0.9532	0.8197	0.4099	0.5941	0.5941
$R=7.0$										
DZ	0.8003	0.9988	0.9942	2.2789	0.1429	0.9892	0.7656	0.3828	0.6177	0.6166
TZ	0.8015	0.9998	0.9970	2.2826	0.1429	0.9922	0.7669	0.3835	0.6192	0.6188
QZ	0.8018	1.0001	0.9980	2.2838	0.1429	0.9932	0.7672	0.3836	0.6195	0.6193
5Z	0.8019	1.0002	0.9983	2.2842	0.1429	0.9935	0.7673	0.3837	0.6196	0.6195
[Q5]	0.8020	1.0003	0.9986	2.2847	0.1429	0.9938	0.7674	0.3837	0.6197	0.6197
$R=10.0$										
DZ	0.7666	0.9987	0.9957	2.1944	0.1000	0.9954	0.7232	0.3616	0.6229	0.6227
TZ	0.7676	0.9997	0.9986	2.1982	0.1000	0.9982	0.7246	0.3623	0.6242	0.6241
QZ	0.7679	0.9999	0.9996	2.1995	0.1000	0.9992	0.7249	0.3624	0.6245	0.6244
5Z	0.7680	1.0000	0.9999	2.1999	0.1000	0.9996	0.7250	0.3625	0.6246	0.6245
[Q5]	0.7681	1.0001	1.0003	2.2004	0.1000	0.9999	0.7251	0.3625	0.6248	0.6247

products of the orbital basis functions constitute a linearly independent set. In such a basis, the FCI density can never be reproduced by a single determinant. In order to reproduce the FCI density the product basis $\eta_\alpha \eta_\beta$ must be linearly dependent, as is the case for a complete one-electron basis set. In practice, for finite basis sets, this is not achieved, although the product linear dependence will occur more rapidly than the linear dependence of the individual functions. This can have some consequences for practical calculations.

First, as observed in Table I for the helium atom with the aug-cc-pVDZ basis set, the gradient tolerance requested may not be achievable when the basis set is small; consequently, we expect the accuracy with which the maximum is obtained to increase with basis-set size. Second, since we introduce the electron-electron interaction as we move along the adiabatic connection, we may expect that obtaining the maximum should become easier with increasing λ. Again this effect is visible in Table I for double- and triple-zeta basis sets, where although the gradient convergence criterion is not quite obtained, the final gradient is lower with increasing λ and is of course trivially obtained when $\lambda=1$. Our observations suggest that a gradient tolerance of 10^{-6} a.u. requires basis sets of cardinal number four or larger, even for these relatively simple two-electron systems.

The iterative procedure in Sec. III provides a method for the determination of the modified external potential v_λ that in combination with the scaled electron-electron interaction operator $\lambda\hat{W}$ yields the physical density ρ. The way in which the corresponding density matrices evolve from the Kohn–Sham to the FCI ones is then clearly illustrated in Fig. 5, since the natural-orbital occupation numbers are the eigenvalues of the density matrices obtained at each coupling strength. The maximization of the generalized Lieb functional of Eq. (3) in a finite basis via the procedure in Sec. III provides the link between the noninteracting and physical systems through a series of partially interacting systems. While the maximum may only be precisely obtained in a

Downloaded 07 Jun 2013 to 193.157.137.211. This article is copyrighted as indicated in the abstract. Reuse of AIP content is subject to the terms at: http://jcp.aip.org/about/rights_and_permissions

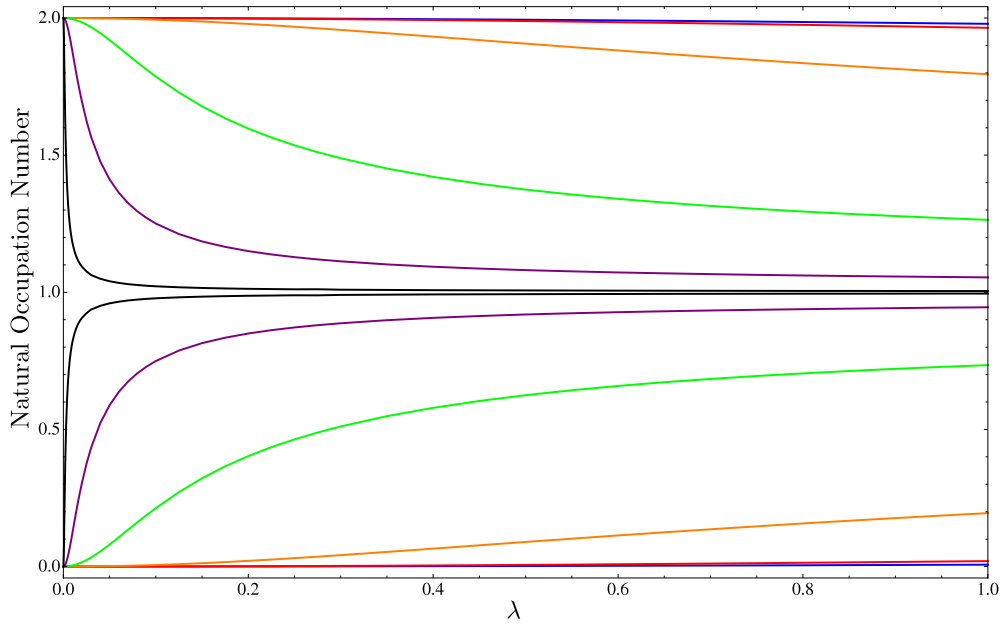

FIG. 5. (Color online) The occupation numbers of the first two natural orbitals as a function of the coupling-strength parameter λ. The upper half of the figure corresponds to the first natural orbital $1\sigma_g$ and the lower half to the second $1\sigma_u$. The individual curves may be distinguished by decreasing the occupation number at $\lambda=1$ with increasing bond length in the upper half and vice versa in the lower half.

complete basis set, we have shown that numerically sufficient accuracy can be achieved to reproduce reasonably accurately the FCI results in the same basis set.

D. The effective potential along the adiabatic connection

The modified external potential v_λ may be decomposed according to Eq. (50). At $\lambda=0$, it is the Kohn–Sham effective potential and at $\lambda=1$ is the usual external potential due to the nuclei. Since the v_{ext} contribution does not vary with λ and the dependence of $v_{J,\lambda}$ is linear, we may wish to examine the exchange-correlation $v_{\text{xc},\lambda}$ and correlation $v_{c,\lambda}$ contributions explicitly. These are given by

$$v_{\text{xc},\lambda}(\mathbf{r}) = (1-\lambda)\int \frac{\rho_0(\mathbf{r}')-\rho(\mathbf{r}')}{|\mathbf{r}-\mathbf{r}'|}d\mathbf{r}' - \frac{(1-\lambda)}{N}\int \frac{\rho_0(\mathbf{r}')}{|\mathbf{r}-\mathbf{r}'|}d\mathbf{r}' + \sum_t b_t g_t(\mathbf{r}) \tag{65}$$

and

$$v_{c,\lambda}(\mathbf{r}) = v_{\text{xc},\lambda}(\mathbf{r}) + \frac{(1-\lambda)}{2}\int \frac{\rho(\mathbf{r}')}{|\mathbf{r}-\mathbf{r}'|}d\mathbf{r}', \tag{66}$$

where ρ_0 is the density used in the calculation of the Fermi–Amaldi reference potential and, in the latter expression, we exploit the fact that for a two-electron system, the exchange potential is $-\frac{1}{2}v_J$. From the discussion in Sec. V C it follows that since in a finite basis set the maximum of the target functional $\mathcal{F}_{\lambda,\mathbf{b}}[\rho]$ cannot generally be precisely obtained, neither can the potential v_λ. This problem has been widely discussed in the literature in relation to the OEP method[63–72] and more recently in the context of constrained-search procedures[73] at $\lambda=0$.

Several procedures have been proposed for dealing with this issue. In the present case, we employ the TSVD method to regularize the Hessian in the optimization procedure. When used in conjunction with an auxiliary basis set for the potential expansion that is the same as the orbital basis, this is sufficient to ensure almost smooth accurate potentials. Typically unphysical oscillations remain only in regions very close to the nuclei. To remove these, we have (for the calculation of the potentials only) utilized the smoothing norm penalty function procedure of Heaton-Burgess *et al.*[72] and Bulat *et al.*[73] with a the regularization parameter set to $\lambda=10^{-5}$ in addition to the TSVD method. This additional constraint lowers the values of the target functional $\mathcal{F}_{\lambda,\mathbf{b}}[\rho]$ obtained in the optimization by less than 10^{-4} a.u. The nonuniqueness of the potential is a consequence of the use of a finite orbital basis set, in which case there is in general no unique mapping between the potential and density as pointed out in Ref. 61. This problem is further exacerbated when the potential expansion and primary orbital basis sets are unbalanced. It is therefore necessary to impose extra constraints on the maximization.

The exchange-correlation and correlation contributions [Eqs. (65) and (66)] calculated with these constraints are presented in Fig. 6 for the helium atom. The potentials were calculated for λ values between 0 and 1 in steps of 0.1. The potentials in Fig. 6(a) show the exchange-correlation contribution, the potentials decreasing with increasing λ. When $\lambda=1$, all the modifying contributions to the external potential are zero. Figure 6(b) shows the correlation-only potentials for the same values of λ. These agree closely with those presented in Ref. 43 for the $\lambda=0$ case. It is known that this contribution does not vary linearly with respect to λ and this is visible. However, it is clear that the correlation contribution to the modified external potential is a very small contribution and so one would expect the Harris–Jones adiabatic

Downloaded 07 Jun 2013 to 193.157.137.211. This article is copyrighted as indicated in the abstract. Reuse of AIP content is subject to the terms at: http://jcp.aip.org/about/rights_and_permissions

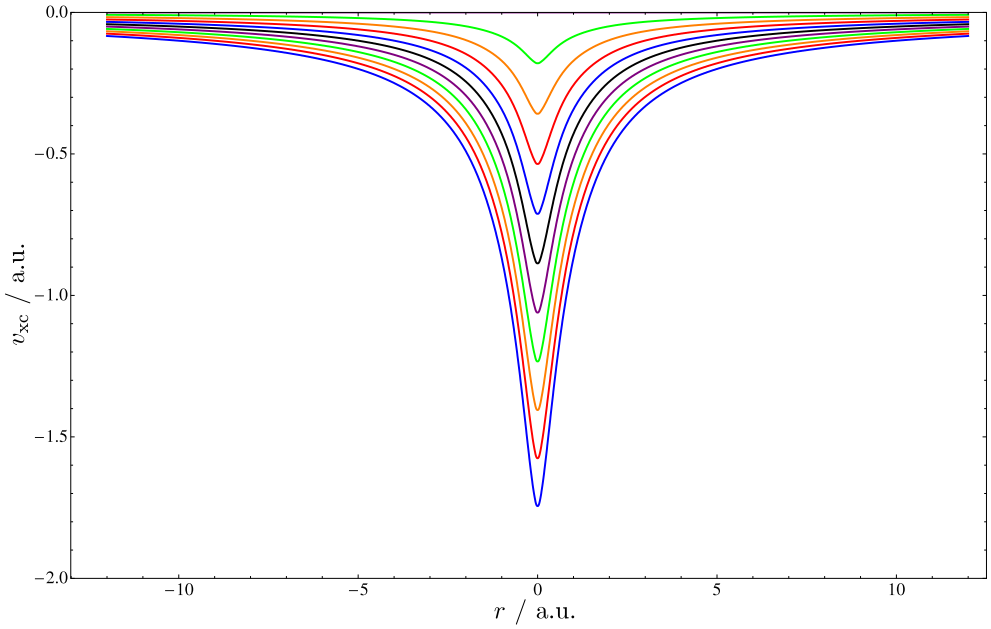

(a) Exchange–Correlation contributions to the modified external potential, $v_{xc,\lambda}$

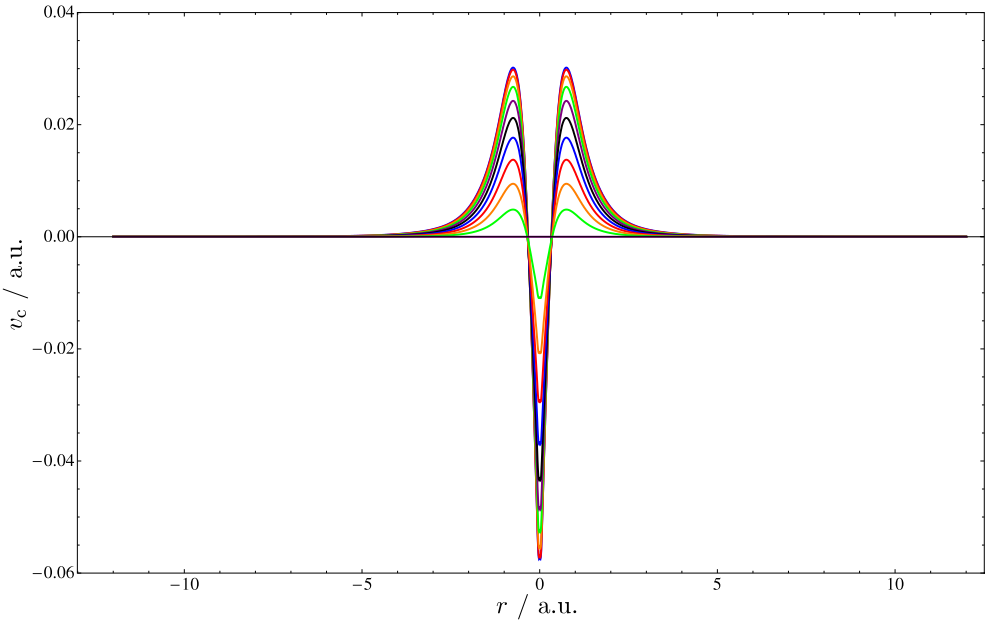

(b) Correlation contributions to the modified external potential, $v_{c,\lambda}$

FIG. 6. (Color online) Exchange-correlation and correlation only contributions to the modifying potential v_λ for $0 \leq \lambda \leq 1$ (in steps of 0.1) for the helium atom.

connection[3] in which the modifying potential is approximated as $v_\lambda = (1-\lambda)v_{\lambda=0} + \lambda v_{\lambda=1}$ to be a good approximation to the adiabatic connections presented in the present work. This was indeed confirmed in the work of Colonna and Savin.[18]

The same procedure can be applied to the H_2 molecule. In this case, the potentials show a similar behavior as λ changes but the size of the correlation potential changes as the bond is stretched. At $R=0.7$ bohr, the correlation potential displays smaller maximum and minimum values than in the helium case, again consistent with a small perturbation. At equilibrium, the maximum and minimum values are similar to those observed for helium. Further stretching the bond results in much larger potentials, which can no longer be regarded as small perturbations. The shape and magnitude of the potentials are consistent with those in Ref. 74. As a consequence, the Harris–Jones adiabatic connection is expected to become less and less accurate with increasing bond length in H_2.

E. Comparison with approximate forms for the adiabatic-connection integrand

A large motivation to study the adiabatic connection is of course the development of more accurate exchange-correlation functionals for use in Kohn–Sham calculations. There have been a number of attempts to develop functionals by explicitly approximating the integrand $\mathcal{W}_{xc,\lambda}[\rho]$ calculated in the present work. The first of these was the half-and-half functional of Becke[75] in which a simple linear interpo-

Downloaded 07 Jun 2013 to 193.157.137.211. This article is copyrighted as indicated in the abstract. Reuse of AIP content is subject to the terms at: http://jcp.aip.org/about/rights_and_permissions

lation between the Hartree–Fock exchange energy functional (the $\mathcal{W}_{xc,0}[\rho]$ value) and an LDA for $\mathcal{W}_{xc,1}[\rho]$ was performed. This yielded exchange-correlation functionals containing 50% Hartree–Fock exchange. It was, however, noted that a somewhat lower percentage could improve the thermochemical performance of the resulting functionals. This seminal functional may be regarded as a precursor to the ubiquitous B3LYP functional[76–80] although, as noted in Ref. 81, the Becke three-parameter functional represents a partial abandonment of the adiabatic-connection idea.

More recently, Ernzerhof proposed the use of a [1/1]-Padé-type form[8] resulting in exchange-correlation functionals in which the Hartree–Fock exchange contribution enters in a nonlinear fashion. This form has also been utilized in the functionals of Mori-Sánchez *et al.*[11] Other approximate forms of note are the two-legged representation of Burke *et al.*[14] and the interaction strength interpolation of Seidl and co-workers,[15,16] the latter of which employs information from the strictly correlated limit of the adiabatic connection ($\lambda=\infty$) to perform an interpolation of $\mathcal{W}_{xc,\lambda}[\rho]$. The fact that some Hartree–Fock-type exchange naturally enters functionals developed from the adiabatic connection provides the motivation for the construction of hybrid functionals, and arguments based on the adiabatic connection have been employed to justify the inclusion of certain amounts of the Hartree–Fock contribution.[9,75]

In our recent works,[23,24] we highlighted the accuracy that can be achieved using relatively simple approximate forms for the integrand $\mathcal{W}_{xc,\lambda}[\rho]$ when the parameters within them are determined using accurate data. In Ref. 24, we compared the performance of nine such forms, six of which were considered in the implementation of new self-consistent density functionals in Ref. 12. When accurate input information was utilized to calculate the parameters in the approximate forms, the Padé form first proposed by Ernzerhof[8] and later employed by Mori-Sánchez *et al.*,[11]

$$\mathcal{W}_{xc,\lambda}^{AC1}[\rho] = a[\rho] + \frac{b[\rho]\lambda}{1+c[\rho]\lambda}, \tag{67}$$

$$E_{xc}^{AC1}[\rho] = a[\rho] + b[\rho]\left(\frac{c[\rho] - \log_e(1+c[\rho])}{c[\rho]^2}\right), \tag{68}$$

$$a[\rho] = \mathcal{W}_{xc,0}[\rho], \tag{69}$$

$$b[\rho] = \mathcal{W}'_{xc,0}[\rho], \tag{70}$$

$$c[\rho] = \frac{\mathcal{W}'_{xc,0}[\rho]}{\mathcal{W}_{xc,1}[\rho] - \mathcal{W}_{xc,0}[\rho]} - 1 \tag{71}$$

and the exponential form proposed in Ref. 12,

$$\mathcal{W}_{xc,\lambda}^{AC6}[\rho] = a[\rho] + b[\rho]\exp(c[\rho]\lambda), \tag{72}$$

$$E_{xc}^{AC6}[\rho] = a[\rho] + \frac{b[\rho]}{c[\rho]}(1-\exp(-c[\rho])), \tag{73}$$

$$a[\rho] = \mathcal{W}_{xc,0}[\rho] - b[\rho], \tag{74}$$

$$b[\rho](1-\exp(\mathcal{W}'_{xc,0}[\rho]/b[\rho])) = \mathcal{W}_{xc,0}[\rho] - \mathcal{W}_{xc,1}[\rho], \tag{75}$$

$$c[\rho] = \frac{\mathcal{W}'_{xc,0}[\rho]}{b[\rho]} \tag{76}$$

were the most accurate in reproducing the FCI exchange-correlation energies of the helium isoelectronic series and the H_2 molecule. In both cases the parameters a, b, and c were calculated using the explicit functionals

$$\mathcal{W}_{xc,0}[\rho] = E_x[\varphi], \tag{77}$$

$$\mathcal{W}'_{xc,0}[\rho] = 2E_c^{GL2}[\varphi], \tag{78}$$

$$\mathcal{W}_{xc,1}[\rho] = \langle\Psi_1|\hat{W}|\Psi_1\rangle - J[\rho], \tag{79}$$

as described in Refs. 23 and 24. We have confirmed that these values reproduce values calculated from our accurate curves to better than 10^{-4} a.u. Here we use the notation AC1 and AC6 to denote the fact that the parameters a, b, and c were determined using this accurate FCI data rather than using density-functional approximations. Both forms show the correct qualitative behavior of the integrand presented in Figs. 2 and 4.

The notable feature of the H_2 dissociation curves calculated using the AC1 form was a small unphysical barrier around $R=5.0$ bohr (see the potential-energy curves in Ref. 24). Although the dissociation of this form is correct and errors relative to the FCI curve are a vast improvement in comparison with those of standard DFT functionals, the presence of this barrier is unsatisfactory. A similar feature was observed in the random phase approximation calculations of Fuchs *et al.*[10]

In the present work, we can now explicitly compare the accurate $\mathcal{W}_{xc,\lambda}[\rho]$ curves with those of the approximate forms. We again employ the extrapolated quantities although the same qualitative behavior is observed for all basis sets. Figure 7 presents the difference between the $\mathcal{W}_{xc,\lambda}^{AC1}[\rho]$ approximate values and the accurate $\mathcal{W}_{xc,\lambda}[\rho]$ integrand.

The integrals of the curves shown are the errors in the exchange-correlation energy obtained from the AC1 form (the accurate curves give the FCI values by construction). At short and equilibrium bond lengths, the error is very small, indicating that the subtle curvature in $\mathcal{W}_{xc,\lambda}[\rho]$ is well reproduced. However, as the bond is stretched and static correlation becomes increasingly important, the curvature of $\mathcal{W}_{xc,\lambda}[\rho]$ grows rapidly. The errors in the exchange-correlation energy given by the AC1 form grow rapidly. Notably, the AC1 form is always above the exact $\mathcal{W}_{xc,\lambda}[\rho]$ except at the noninteracting and physical points (which are the same by construction). The error (the integrals of the curves shown in the inset) is greatest at $R=5.0$ bohr, consistent with the potential-energy curves presented in Ref. 24.

It is noteworthy that the use of accurate input information in the calculation of approximate adiabatic-connection curves is essential, especially for the derivatives of $\mathcal{W}_{xc,\lambda}[\rho]$ at $\lambda=0$. For example, in Ref. 11 an approximate gradient based on the meta-GGA functional form of Refs. 82 and 83

Downloaded 07 Jun 2013 to 193.157.137.211. This article is copyrighted as indicated in the abstract. Reuse of AIP content is subject to the terms at: http://jcp.aip.org/about/rights_and_permissions

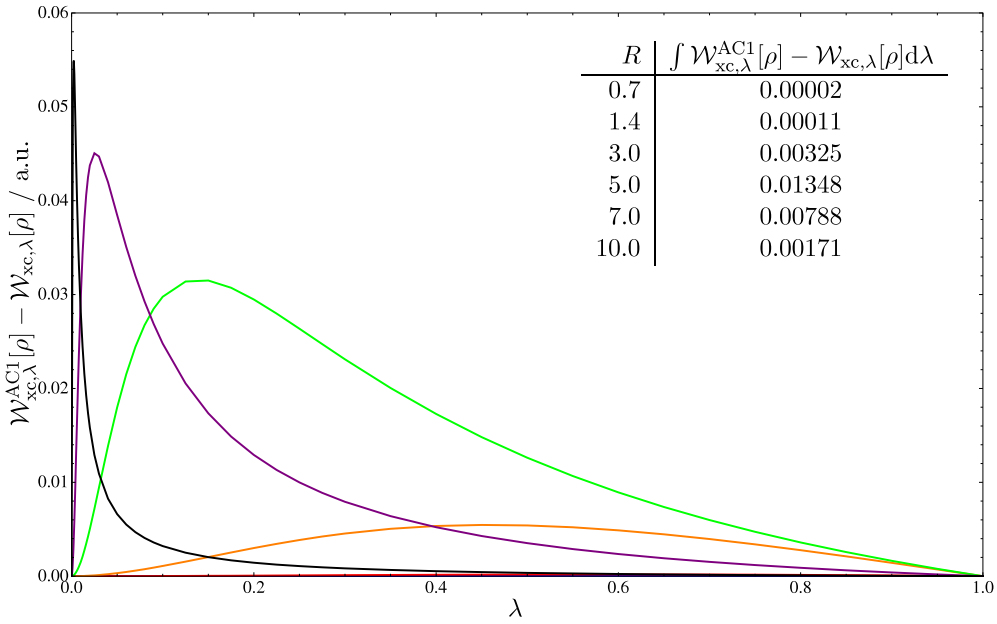

FIG. 7. (Color online) Differences between the approximate Padé form AC1 and the accurate adiabatic-connection curves of the present work. The inset presents the errors. The plots for the shortest two bond lengths are barely visible. The curves may be distinguished by noting that their maxima move to smaller λ for increasing R.

was employed in the implementation of a self-consistent functional using the Padé-type form and the resulting dissociation curves for H_2 are of B3LYP quality.[23] Also, in Ref. 12 the self-consistent implementation of several forms was investigated with approximate density functionals for the input parameters and little difference in their performance was observed.

In our recent work, we highlighted the success of the AC6 form in eliminating the unphysical barrier in the H_2 dissociation observed with the AC1 form. It is important to understand if this is due to some error cancellation or if the form chosen is actually a better approximation to the adiabatic-connection curve. In Fig. 8, we present explicitly the differences between the AC6 approximate values and the accurate $\mathcal{W}_{\mathrm{xc},\lambda}[\rho]$ integrand. The errors observed at all geometries are a great improvement over the AC1 form, as exhibited by the more compact scale of the y axis. However, the curves are no longer all above the exact one for this approximate form. Again, the noninteracting and physical points agree by construction but, for this form, a crossing can occur at intermediate values of λ. At short and equilibrium bond lengths, errors are minimal; as the bond is stretched to $R=3.0$ bohr, a positive error is introduced. Further increasing the bond length results in a certain degree of error can-

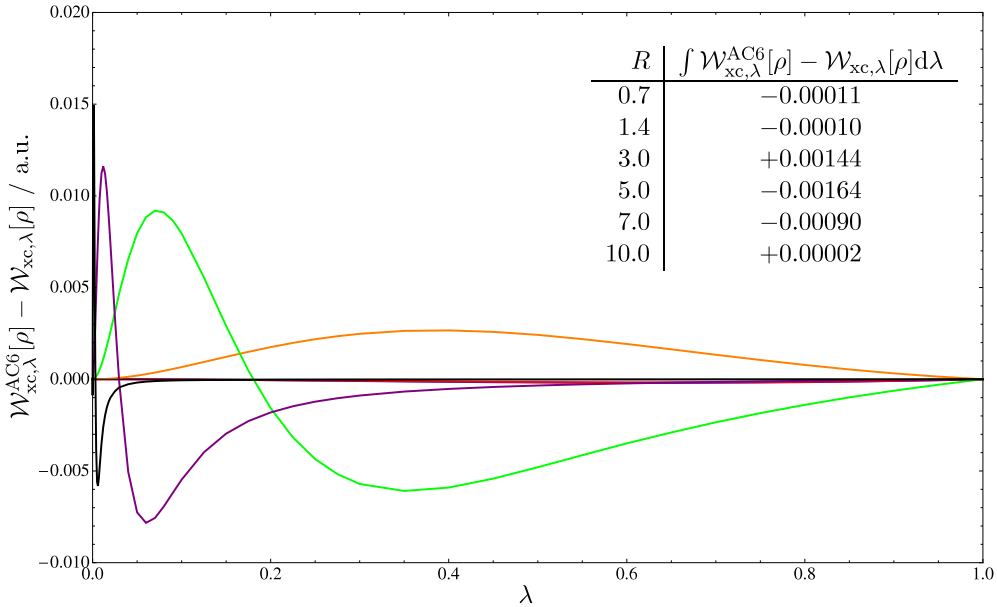

FIG. 8. (Color online) Differences between the exponential approximate form AC6 and the accurate adiabatic-connection curves calculated in the present work. The inset presents the errors. Again the curves for the shortest two bond lengths are barely visible. The curves may be distinguished by noting that their maxima move to smaller λ for increasing R.

Downloaded 07 Jun 2013 to 193.157.137.211. This article is copyrighted as indicated in the abstract. Reuse of AIP content is subject to the terms at: http://jcp.aip.org/about/rights_and_permissions

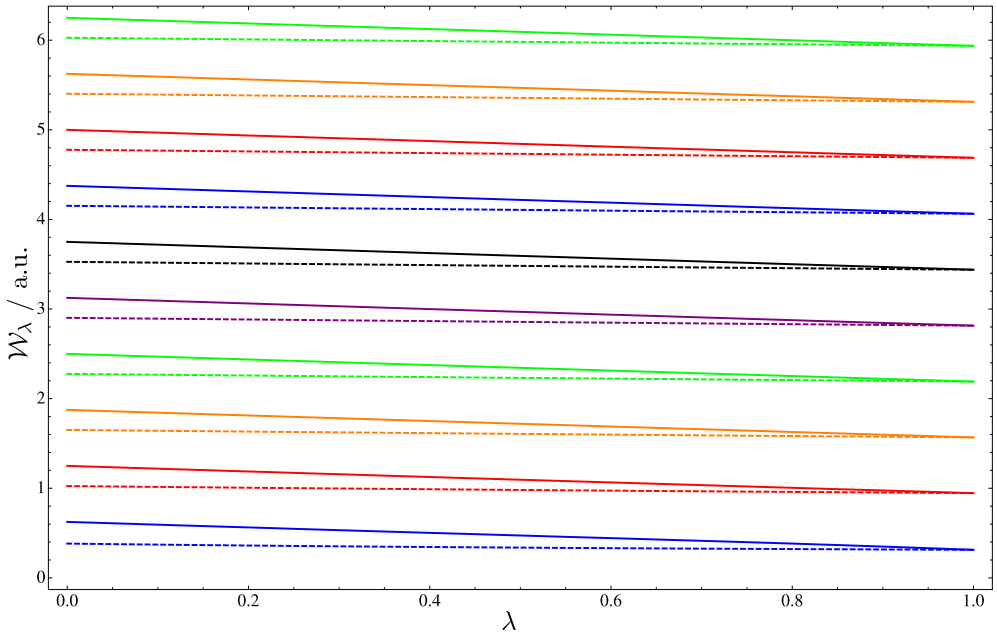

FIG. 9. (Color online) Plots of the adiabatic connection integrands with a fixed potential $\mathcal{W}_\lambda[v]$ (solid lines) and a fixed density $\mathcal{W}_\lambda[\rho]$ (dashed lines) for the helium isoelectronic series. The curves may be distinguished by noting that they become more positive with increasing nuclear charge $1 \leq Z \leq 10$.

cellation as the approximate adiabatic-connection curve is initially above the exact one and then later falls below it before rising again to meet the exact value at $\lambda = 1$. As in the AC1 case, further stretching the bond length results in a localization of the error to the low λ end of the adiabatic connection. The analysis presented here is consistent with the potential-energy curves presented in Ref. 24. This is one area in which we hope the present procedure will prove very useful—the testing of new approximate density functional forms and the detection of error cancellation.

F. Potential-fixed adiabatic-connection curves

For the density-fixed adiabatic connection, the determination of the potential v_λ was a maximization problem that required the implementation of a new iterative scheme. For the potential-fixed adiabatic connection, the situation is more straightforward—namely, since $v_1 = v_{\text{ext}}$, we simply need to perform FCI calculations in which we use the usual external potential with a scaled electron-electron interaction. Furthermore, the cost is substantially lower as the optimization of the wave function is carried out only once—no iterative refinement of the potential is required. We have applied this procedure to the helium isoelectronic series and the H_2 molecule as was done for the density-fixed connection. In Fig. 9, we present plots of $\mathcal{W}_\lambda[v]$ and $\mathcal{W}_\lambda[\rho]$ as a function of λ for the helium isoelectronic series; likewise, in Fig. 10, plots are presented for the H_2 molecule at the same geometries considered previously. In Table V, the integrals of these basis-set extrapolated curves are presented along with the zero-order energies.

Upon integration, the density-fixed adiabatic-connection curves provide the Coulomb, exchange, and correlation contributions corresponding to the physical density in addition to the correlation corrections to the noninteracting kinetic energy again associated with the physical density. Of these contributions the Coulomb part is by far the largest; the kinetic correction is a small positive contribution, smaller than or equal in magnitude to the correlation contribution. These curves are presented in Figs. 9 and 10 as dashed lines and are simply the plots of Figs. 2 and 4 with the constant Coulomb and exchange contributions added. By contrast, the potential-fixed adiabatic-connection curves when integrated provide the Coulomb, exchange, correlation, and kinetic-energy corrections to the BN system and are presented as solid lines in Figs. 9 and 10. Since the density in this case changes along the adiabatic connection, the Coulomb and exchange contributions are no longer constant.

The Coulomb correction in the present case is dominant and results in all of the curves having positive values. These increase with Z for the helium isoelectronic series in Fig. 9 and increase as the internuclear separation R decreases for the H_2 molecule in Fig. 10. Comparing the density- and potential-fixed adiabatic connections, we note that these are both monotonically decreasing curves, which coincide at $\lambda = 1$ since the fully interacting density matrices are identical $\hat{\gamma}_1^v = \hat{\gamma}_1^\rho$. Monotonicity is easily shown in both cases using the variation principle. We also note that the potential-fixed curve is always above the corresponding density-fixed curve. To understand this behavior, we note that the zero-order BN approximation, by neglecting all electronic interactions, provides an electronic density that is more compact than the true density, resulting in a two-electron interaction that is higher than that of the density-fixed adiabatic interaction. For the stretched H_2 molecule, the effects of strong static correlation become evident as the Coulomb repulsion between the electrons decays, resulting in the characteristic curvature of the largest three internuclear separations. Integration of the curves and addition to the BN energy give excellent agreement with the FCI energies, as shown in Table V.

Downloaded 07 Jun 2013 to 193.157.137.211. This article is copyrighted as indicated in the abstract. Reuse of AIP content is subject to the terms at: http://jcp.aip.org/about/rights_and_permissions

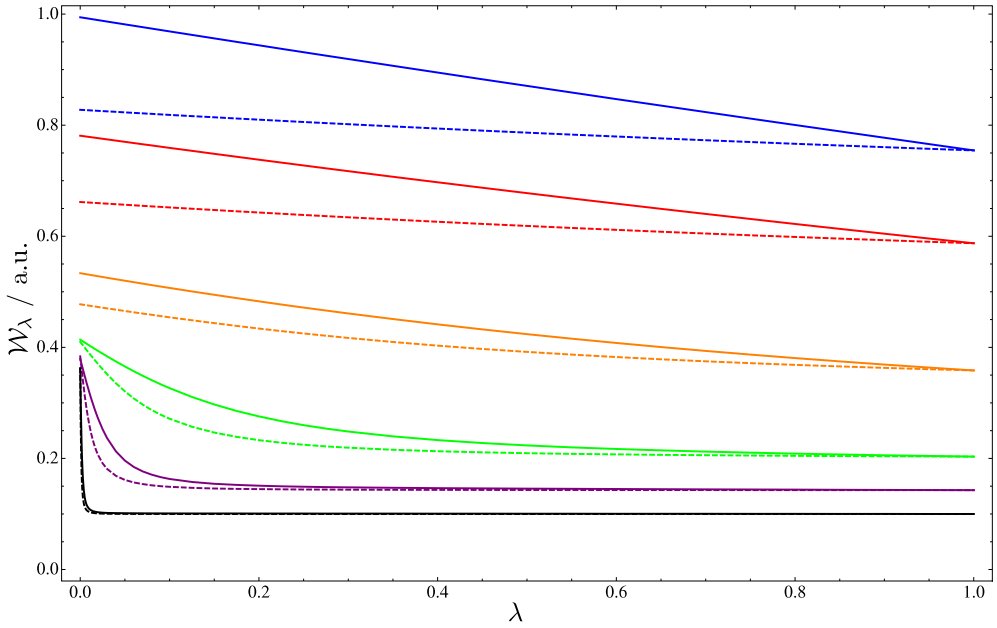

FIG. 10. (Color online) Plots of the adiabatic-connection integrands with a fixed potential $\mathcal{W}_\lambda[v]$ (solid lines) and a fixed density $\mathcal{W}_\lambda[\rho]$ (dashed lines) for the H_2 molecule at a range of internuclear separations. $R=0.7$, 1.4, 3.0, 5.0, 7.0, and 10.0 bohr. The curves can be distinguished by noting that at $\lambda=1$ the values of the integrands fall with increasing bond length.

VI. CONCLUSIONS

The performance of an iterative procedure for the calculation of the universal Lieb functional generalized to arbitrary electron-electron interaction strengths has been examined. Specifically, we have applied the procedure to the helium isoelectronic series and the H_2 molecule, calculating the universal density functional $F_\lambda[\rho]$ and energies from high-quality FCI wave functions in large basis sets. Comparing first- and second-order schemes for the optimization of the Lieb functional, the latter was found to offer significantly better convergence with the extra effort incurred in evaluating the static density-density response function offset by a large reduction in the number of iterations required.

The procedure was then applied to the helium isoelectronic series. The adiabatic-connection curves are known to become close to linear as the nuclear charge increases and the high-density limit is approached. This behavior was demonstrated explicitly in Fig. 2. The exact value of the exchange-correlation energy for the FCI density was then calculated and compared with that obtained by the integration of our accurate adiabatic-connection curves. Agreement in all cases was excellent, demonstrating the accuracy of the iterative procedure for a variety of densities.

TABLE V. Values of the BN electronic energy and the integral of the potential-fixed adiabatic-connection curves. The sum of the zero-order and correction terms is also presented for comparison with the FCI values. All values are for basis-set limit quantities in atomic units.

Species	R	E_0	$\int\mathcal{W}_\lambda d\lambda$	$E_0+\int\mathcal{W}_\lambda d\lambda$	E^{FCI}
H^-		−1.0000	0.4724	−0.5277	−0.5277
He		−4.0000	1.0963	−2.9038	−2.9038
Li^+		−9.0000	1.7203	−7.2796	−7.2796
Be^{2+}		−16.0000	2.3446	−13.6554	−13.6554
B^{3+}		−25.0000	2.9690	−22.0311	−22.0311
C^{4+}		−36.0000	3.5938	−32.4064	−32.4064
N^{5+}		−49.0000	4.2186	−44.7816	−44.7816
O^{6+}		−64.0000	4.8433	−59.1568	−59.1568
F^{7+}		−81.0000	5.4681	−75.5321	−75.5321
Ne^{8+}		−100.0000	6.0931	−93.9069	−93.9069
H_2	0.7	−1.7944	0.8720	−0.9225	−0.9225
	1.4	−1.8545	0.6798	−1.1747	−1.1747
	3.0	−1.4886	0.4312	−1.0574	−1.0574
	5.0	−1.2489	0.2451	−1.0039	−1.0039
	7.0	−1.1541	0.1538	−1.0003	−1.0003
	10.0	−1.1012	0.1011	−1.0001	−1.0001

Downloaded 07 Jun 2013 to 193.157.137.211. This article is copyrighted as indicated in the abstract. Reuse of AIP content is subject to the terms at: http://jcp.aip.org/about/rights_and_permissions

We then shifted our attention to the H_2 molecule which may be regarded as a prototypical system for bond dissociation. The accurate adiabatic-connection curves for a variety of bond lengths were calculated and again exchange-correlation energies obtained by integration were compared with accurate FCI values. It was noted that at longer bond lengths where static correlation dominates, the calculated values of the adiabatic-connection curves are insensitive to the choice of basis set. We then discussed in some detail the relationship between the Kohn–Sham orbitals and the natural orbitals as a function of the coupling strength, making clear the relationship between the curvature of the adiabatic connection and the degree of static correlation.

The exchange-correlation contributions to the modified external potential v_λ as a function of electron-electron interaction strength were examined and the need to apply a smoothing procedure to obtain accurate potentials was discussed. It was shown that the correlation potentials obtained agree well with those in previous studies. The alternative Harris–Jones adiabatic connection was then discussed, showing that the agreement with the connection in the present work is expected to be good when the correlation potential is a small perturbation, as in the case of the helium isoelectronic series, but much worse when the perturbation is large, such as in the case of stretched H_2.

The accurate adiabatic-connection curves were then used to highlight the strengths and weaknesses of two recently investigated approximate forms. This is an area in which the presented procedure should prove very useful in the future—the investigation of new exchange-correlation functionals and the detection and diagnosis of errors. Indeed, a degree of error cancellation was found in the AC6 form.

Finally, we compared the usual adiabatic connection based on a fixed density with the adiabatic connection based on a fixed potential, relating the BN approximation to the fully interacting system. The adiabatic-connection curves were found to be similar in two cases, both decreasing monotonically toward the same value at full interaction strength, the potential-fixed curve always being higher than the density-fixed curve.

We close by considering some directions for future research. The linear adiabatic-connection formalism discussed throughout the present work may easily be generalized, as discussed in Ref. 84, to a general electronic interaction operator resulting in nonlinear adiabatic connections. Various alternatives for the operator to be used exist and some investigations have been carried out by Savin and co-workers.[21,85,86] The generalization of the scheme presented here is straightforward and work in this direction is already underway. Application of this scheme to other molecular systems is also already in progress, in this case the coupled-cluster singles-doubles-perturbative-triples densities will be used to provide an approximation to the physical density for systems with more than two electrons.

Another aspect which remains to be investigated is calculation of the adiabatic connection beyond the physical interaction strength. A great deal of work has been done by Seidl and co-workers[16,87–90] for strictly correlated electrons ($\lambda=\infty$). The procedure investigated here can be applied to values of λ beyond the physical interaction strength. The usefulness of the procedure in this context remains to be established. Other areas in which adiabatic-connection calculations may be illuminating are the many-electron self-interaction error[13,91,92] and the description of van der Waals systems and dispersion interactions. Work on the latter is currently in progress.

ACKNOWLEDGMENTS

This work has been supported by the Norwegian Research Council through Grant No. 171185 (A.M.T.) and the CeO Centre for Theoretical and Computational Chemistry through Grant No. 179568/V30. The authors thank R. Dragsreth for technical assistance. They also thank P. Jørgensen, J. Olsen, D. J. Tozer, and M. J. G. Peach for helpful discussions and E. Carter for useful comments on preliminary results of this work presented at the Norwegian Theoretical Chemistry meeting in Trondheim.

[1] E. H. Lieb, Int. J. Quantum Chem. **24**, 243 (1983).
[2] R. F. Nalewajski and R. G. Parr, J. Chem. Phys. **77**, 399 (1982).
[3] J. Harris and R. O. Jones, J. Phys. F: Met. Phys. **4**, 1170 (1974).
[4] D. C. Langreth and J. P. Perdew, Solid State Commun. **17**, 1425 (1975).
[5] O. Gunnarsson and B. I. Lundqvist, Phys. Rev. B **13**, 4274 (1976).
[6] O. Gunnarsson and B. I. Lundqvist, Phys. Rev. B **15**, 6006 (1977).
[7] D. C. Langreth and J. P. Perdew, Phys. Rev. B **15**, 2884 (1977).
[8] M. Ernzerhof, Chem. Phys. Lett. **263**, 499 (1996).
[9] M. Ernzerhof, J. P. Perdew, and K. Burke, Int. J. Quantum Chem. **64**, 285 (1997).
[10] M. Fuchs, Y.-M. Niquet, X. Gonze, and K. Burke, J. Chem. Phys. **122**, 094116 (2005).
[11] P. Mori-Sánchez, A. J. Cohen, and W. Yang, J. Chem. Phys. **124**, 091102 (2006).
[12] A. J. Cohen, P. Mori-Sánchez, and W. Yang, J. Chem. Phys. **127**, 034101 (2007).
[13] A. J. Cohen, P. Mori-Sánchez, and W. Yang, J. Chem. Phys. **126**, 191109 (2007).
[14] K. Burke, M. Ernzerhof, and J. P. Perdew, Chem. Phys. Lett. **265**, 115 (1997).
[15] M. Seidl, J. P. Perdew, and S. Kurth, Phys. Rev. Lett. **84**, 5070 (2000).
[16] M. Seidl, Int. J. Quantum Chem. **91**, 145 (2003).
[17] D. P. Joubert and G. P. Srivastava, J. Chem. Phys. **109**, 5212 (1998).
[18] F. Colonna and A. Savin, J. Chem. Phys. **110**, 2828 (1999).
[19] D. Frydel, W. M. Terilla, and K. Burke, J. Chem. Phys. **112**, 5292 (2000).
[20] A. Savin, F. Colonna, and M. Allavena, J. Chem. Phys. **115**, 6827 (2001).
[21] R. Pollet, F. Colonna, T. Leininger, H. Stoll, H.-J. Werner, and A. Savin, Int. J. Quantum Chem. **91**, 84 (2003).
[22] Q. Wu and W. Yang, J. Chem. Phys. **118**, 2498 (2003).
[23] M. J. G. Peach, A. M. Teale, and D. J. Tozer, J. Chem. Phys. **126**, 244104 (2007).
[24] M. J. G. Peach, A. M. Miller, A. M. Teale, and D. J. Tozer, J. Chem. Phys. **129**, 064105 (2008).
[25] O. Sinanoğlu, Phys. Rev. **122**, 493 (1961).
[26] A. Gorling and M. Levy, Phys. Rev. B **47**, 13105 (1993).
[27] A. Gorling and M. Levy, Phys. Rev. A **50**, 196 (1994).
[28] DALTON, a molecular electronic structure program, release 2.0, 2005, see http://www.kjemi.uio.no/software/dalton/dalton.html.
[29] A. Zangwill and P. Soven, Phys. Rev. A **21**, 1561 (1980).
[30] M. J. Stott and E. Zaremba, Phys. Rev. A **21**, 12 (1980).
[31] R. G. Parr and W. Yang, *Density-Functional Theory of Atoms and Molecules* (Oxford Science Publications, Oxford, 1989).
[32] T. Helgaker, P. Jørgensen, and J. Olsen, *Modern Electronic-Structure Theory* (Wiley, New York, 2000).
[33] O. Christiansen, P. Jørgensen, and C. Hättig, Int. J. Quantum Chem. **68**, 1 (1998).
[34] Q. Wu and W. Yang, J. Theor. Comput. Chem. **2**, 627 (2003).
[35] T. H. Dunning, Jr., J. Chem. Phys. **90**, 1007 (1989).
[36] R. A. Kendall, T. H. Dunning, Jr., and R. J. Harrison, J. Chem. Phys. **96**, 6796 (1992).

Downloaded 07 Jun 2013 to 193.157.137.211. This article is copyrighted as indicated in the abstract. Reuse of AIP content is subject to the terms at: http://jcp.aip.org/about/rights_and_permissions

[37] D. E. Woon and T. H. Dunning, Jr., J. Chem. Phys. **100**, 2975 (1994).
[38] E. Fermi and E. Amaldi, Mem. Accad. Italia **6**, 117 (1934); reproduced in E. Fermi "Collected Papers (Note e Memorie)", loc. cit., as art. No. 82.
[39] A. M. Teale, A. J. Cohen, and D. J. Tozer, J. Chem. Phys. **126**, 074101 (2007).
[40] T. Heaton-Burgess, A. J. Cohen, W. Yang, and E. R. Davidson, J. Chem. Phys. **128**, 114702 (2008).
[41] MATHEMATICA, Version 6.0.3.0.,Wolfram Research, Inc., Champaign, Illinois (2008).
[42] A. Halkier, T. Helgaker, P. Jørgensen, W. Klopper, H. Koch, J. Olsen, and A. K. Wilson, Chem. Phys. Lett. **286**, 243 (1998).
[43] C. J. Umrigar and X. Gonze, Phys. Rev. A **50**, 3827 (1994).
[44] A. A. Jarzecki and E. R. Davidson, Phys. Rev. A **58**, 1902 (1998).
[45] P. M. W. Gill, D. L. Crittenden, D. P. O'Neill, and N. A. Besley, Phys. Chem. Chem. Phys. **8**, 15 (2006).
[46] J. Katriel, S. Roy, and M. Springborg, J. Chem. Phys. **123**, 104104 (2005).
[47] J. P. Perdew, E. R. McMullen, and A. Zunger, Phys. Rev. A **23**, 2785 (1981).
[48] D. E. Woon and T. H. Dunning, Jr., J. Chem. Phys. **103**, 4572 (1995).
[49] M. Levy and J. Perdew, Phys. Rev. A **32**, 2010 (1985).
[50] M. Levy, in *Density Functional Theory*, edited by E. K. U. Gross and R. M. Dreizler (Plenum, New York, 1995), Vol. 337.
[51] C.-J. Huang and C. J. Umrigar, Phys. Rev. A **56**, 290 (1997).
[52] T. K. Whittingham and K. Burke, J. Chem. Phys. **122**, 134108 (2005).
[53] W. Kolos and C. C. J. Roothaan, Rev. Mod. Phys. **32**, 219 (1960).
[54] E. J. Baerends, Phys. Rev. Lett. **87**, 133004 (2001).
[55] M. Grüning, O. V. Gritsenko, and E. J. Baerends, J. Chem. Phys. **118**, 7183 (2003).
[56] O. Gritsenko and E. J. Baerends, Int. J. Quantum Chem. **106**, 3167 (2006).
[57] W. Kolos, K. Szalewicz, and H. J. Monkhorst, J. Chem. Phys. **84**, 3278 (1986).
[58] W. Kolos and J. Rychlewski, J. Chem. Phys. **98**, 3960 (1993).
[59] T. L. Gilbert, Phys. Rev. B **12**, 2111 (1975).
[60] G. Baumann and R. Duscher, Z. Phys. B: Condens. Matter **69**, 243 (1987).
[61] J. E. Harriman, Phys. Rev. A **27**, 632 (1983).
[62] J. E. Harriman, Phys. Rev. A **34**, 29 (1986).
[63] S. Hirata, S. Ivanov, I. Grabowski, R. J. Bartlett, K. Burke, and J. D. Talman, J. Chem. Phys. **115**, 1635 (2001).
[64] R. J. Bartlett, I. Grabowski, S. Hirata, and S. Ivanov, J. Chem. Phys. **122**, 034104 (2005).
[65] V. N. Staroverov, G. E. Scuseria, and E. R. Davidson, J. Chem. Phys. **125**, 081104 (2006).
[66] V. N. Staroverov, G. E. Scuseria, and E. R. Davidson, J. Chem. Phys. **124**, 141103 (2006).
[67] D. Rohr, O. V. Gritsenko, and E. J. Baerends, J. Mol. Struct.: THEOCHEM **762**, 193 (2006).
[68] A. Heßelmann, A. W. Götz, F. Della Sala, and A. Görling, J. Chem. Phys. **127**, 054102 (2007).
[69] C. Kollmar and M. Filatov, J. Chem. Phys. **127**, 114104 (2007).
[70] D. P. Joubert, J. Chem. Phys. **127**, 244104 (2007).
[71] C. Kollmar and M. Filatov, J. Chem. Phys. **128**, 064101 (2008).
[72] T. Heaton-Burgess, F. A. Bulat, and W. Yang, Phys. Rev. Lett. **98**, 256401 (2007).
[73] F. A. Bulat, T. Heaton-Burgess, A. J. Cohen, and W. Yang, J. Chem. Phys. **127**, 174101 (2007).
[74] M. A. Buijse, E. J. Baerends, and J. G. Snijders, Phys. Rev. A **40**, 4190 (1989).
[75] A. D. Becke, J. Chem. Phys. **98**, 1372 (1993).
[76] A. D. Becke, Phys. Rev. A **38**, 3098 (1988).
[77] C. Lee, W. Yang, and R. G. Parr, Phys. Rev. B **37**, 785 (1988).
[78] A. D. Becke, J. Chem. Phys. **98**, 5648 (1993).
[79] S. H. Vosko, L. Wilk, and M. Nusair, Can. J. Phys. **58**, 1200 (1980).
[80] P. J. Stephens, F. J. Devlin, C. F. Chabalowski, and M. J. Frisch, J. Phys. Chem. **98**, 11623 (1994).
[81] M. Levy, N. H. March, and N. C. Handy, J. Chem. Phys. **104**, 1989 (1996).
[82] J. M. Tao, J. P. Perdew, V. N. Staroverov, and G. E. Scuseria, Phys. Rev. Lett. **91**, 146401 (2003).
[83] J. P. Perdew, J. Tao, V. N. Staroverov, and G. E. Scuseria, J. Chem. Phys. **120**, 6898 (2004).
[84] W. Yang, J. Chem. Phys. **109**, 10107 (1998).
[85] J. Toulouse, F. Colonna, and A. Savin, Phys. Rev. A **70**, 062505 (2004).
[86] J. Toulouse, F. Colonna, and A. Savin, Mol. Phys. **103**, 2725 (2005).
[87] M. Seidl, J. P. Perdew, and S. Kurth, Phys. Rev. A **62**, 012502 (2000).
[88] M. Seidl, J. P. Perdew, and M. Levy, Phys. Rev. A **59**, 51 (1999).
[89] M. Seidl, P. Gori-Giorgi, and A. Savin, Phys. Rev. A **75**, 042511 (2007).
[90] M. Seidl, Phys. Rev. A **60**, 4387 (1999).
[91] A. Ruzsinszky, J. P. Perdew, G. I. Csonka, O. A. Vydrov, and G. E. Scuseria, J. Chem. Phys. **126**, 104102 (2007).
[92] P. Mori-Sánchez, A. J. Cohen, and W. Yang, J. Chem. Phys. **125**, 201102 (2006).

Downloaded 07 Jun 2013 to 193.157.137.211. This article is copyrighted as indicated in the abstract. Reuse of AIP content is subject to the terms at: http://jcp.aip.org/about/rights_and_permissions